



Multiple remote sensing data sources to assess spatio-temporal patterns of fire incidence over Campos Amazônicos Savanna Vegetation Enclave (Brazilian Amazon)

Daniel Borini Alves ^{*}, Fernando Pérez-Cabello

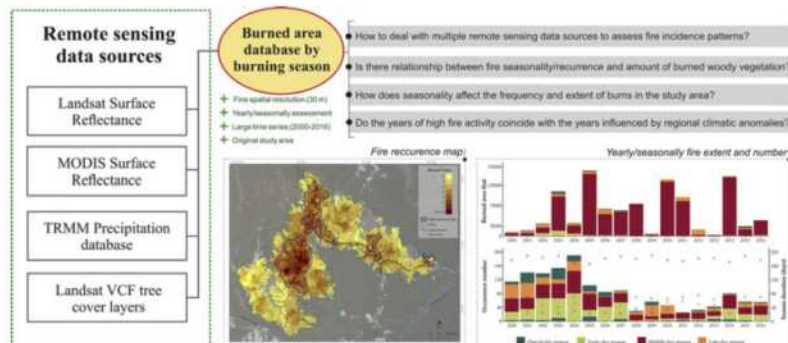
University of Zaragoza, Department of Geography and Land Management, Geoforest-IUCA Group, Calle Pedro Cerbuna, 12, 50009 Zaragoza, Spain



HIGHLIGHTS

- Is the first study that report fire incidence patterns over a savanna enclave of the Brazilian Amazon
- Fire recurrence and seasonality were analyzed using all Landsat-MODIS coincident series.
- 1.03 million ha was burned in the last 17 years (almost 2.5 times its enclave area).
- Middle dry season fires represent 86% of the total burned areas and 32% of fire occurrences.
- Higher density tree surfaces were more significantly affected by fire during the middle dry season.

GRAPHICAL ABSTRACT



ARTICLE INFO

Article history:

Received 2 April 2017
Received in revised form 19 May 2017
Accepted 20 May 2017
Available online 25 May 2017

Editor: D. Barcelo

Keywords:

Fire history
Remote sensing
Seasonality
Conservation units
Savanna enclave
Brazilian Amazon

ABSTRACT

Fire activity plays an important role in the past, present and future of Earth system behavior. Monitoring and assessing spatial and temporal fire dynamics have a fundamental relevance in the understanding of ecological processes and the human impacts on different landscapes and multiple spatial scales. This work analyzes the spatio-temporal distribution of burned areas in one of the biggest savanna vegetation enclaves in the southern Brazilian Amazon, from 2000 to 2016, deriving information from multiple remote sensing data sources (Landsat and MODIS surface reflectance, TRMM pluviometry and Vegetation Continuous Field tree cover layers). A fire scars database with 30 m spatial resolution was generated using a Landsat time series. MODIS daily surface reflectance was used for accurate dating of the fire scars. TRMM pluviometry data were analyzed to dynamically establish time limits of the yearly dry season and burning periods. Burned area extent, frequency and recurrence were quantified comparing the results annually/seasonally. Additionally, Vegetation Continuous Field tree cover layers were used to analyze fire incidence over different types of tree cover domains. In the last seventeen years, 1.03 million ha were burned within the study area, distributed across 1432 fire occurrences, highlighting 2005, 2010 and 2014 as the most affected years. Middle dry season fires represent 86.21% of the total burned areas and 32.05% of fire occurrences, affecting larger amount of higher density tree surfaces than other burning periods. The results provide new insights into the analysis of burned areas of the neotropical savannas, spatially and statistically reinforcing important aspects linked to the seasonality patterns of fire incidence in this landscape.

© 2017 Elsevier B.V. All rights reserved.

^{*} Corresponding author.

E-mail addresses: dborini@unizar.es, fcabello@unizar.es (D.B. Alves).

1. Introduction

Fire is one of the major factors in the dynamic of ecosystem processes playing a key role in Earth system behavior (Bond et al., 2005). Human-induced fires have profoundly influenced fire regime alterations worldwide, largely by increasing fire frequency and destructiveness to ecosystems (Pausas and Keeley, 2009). On a global scale, tropical savannas are the most fire-prone biome and the largest source of atmospheric emissions from biomass burning (Pereira, 2003). The Brazilian neotropical savanna (Cerrado), considered as a global biodiversity hotspot, occupies over 2 million km² and is the second largest biome in the country after the Amazon (Cavalcanti and Joly, 2002). The transition areas between Cerrado and Amazon, also known as the 'Arc of Deforestation and Fire of the Legal Amazon', are the region most frequently affected by fire in the last decades within Brazilian territory (Schroeder et al., 2009; Silva Cardozo et al., 2011).

According to paleoclimatic and paleo-vegetational studies, fire has been burning tropical savannas of South America more than 32,000 years ago (Ledru, 2002; Salgado-Labouriau and Ferraz-Vicentini, 1994), before the presence of man, which demonstrates that natural fire regimes influences in the Cerrado formation, categorized as fire-dependent/influenced landscape (Hardesty et al., 2005). In this type of landscape, natural fire regimes are mainly associated to the occurrence of lightning during the wet season (Ramos-Neto and Pivello, 2000), generally resulting in low intensity burns that plays an important role for nutrient cycling, diversity maintenance and habitat structure (Pivello, 2011). However, the anthropic activities had a significant impact on the increase of fire recurrence in the last decades, directly influencing the alteration of these environments (Goldammer, 1993). High fire frequency or even seasonality alteration of burns are associated with severe impacts on biosphere, pedosphere and atmosphere components (Pausas and Keeley, 2009). Regarding vegetation, frequent fires impact on reduction of nutrient stock and total biomass, especially in relation to tree and shrub formations, which may result in the exclusion of vegetal species more sensitive to fire (Moreira, 2000; Hoffmann and Moreira, 2002), as well as fauna species (Silveira et al., 1999). The incidence of frequent and high temperatures can lead to altered physical and chemical soil characteristics, favoring high rates of erosion and soil losses (Certini, 2005). The total greenhouse gas emissions to the atmosphere from the combustion of fuel loads have also a relevant impact (Levine et al., 1995; Bowman et al., 2010).

Human influences on fire regimes occur directly and indirectly. On the one hand, a direct increase in the number of ignitions is mainly associated with clearing of areas for pasture, land preparation for agriculture and animal attraction for hunting, where fire often gets out of control and generates large forest fires. On the other hand, the changes promoted in the landscape, such as construction of roads and introduction of new vegetation species may be related to the increase of susceptibility to fire on certain areas (Hardesty et al., 2005). In the perspective of anthropogenic influences on climate change, possible extensions of drought seasons may increase the exposure of these areas to the fire risk. In the Cerrado-Amazon transition areas, increase in burned areas is closely related to the last-decades changes in land use and land cover (Eva and Lambin, 2000; Ometto et al., 2016), mainly associated with the expansion of crop and pasture areas, road and communication network construction and population density growth.

In this context, fire activity monitoring is an essential procedure in order to answer purely scientific questions associated with understanding of ecological processes and the human impacts in multiple spatial scales of analysis. Furthermore, it generates valuable information from the point of view of land management, supporting strategic alternatives for biodiversity and soil conservation and reduction of carbon emissions. In Brazil, there is an urgent need in national fire policy (Durigan and Ratter, 2016) defining guidelines and implementing strategies for fire management plans, since this issue is still little considered in the scope of Brazilian conservation policies.

Remote sensing is an essential source allowing generation of systematic information at different spatial and temporal scales necessary for monitoring and better understanding of fire affected areas (Giglio et al., 2010; Pereira, 2003). It provides global coverage and multitemporal assessment, supporting pre- and post-fire studies ranging from the generation of risk models (Chuvienco et al., 2010; Maeda et al., 2009) to the analysis of regeneration processes (Röder et al., 2008; Van Leeuwen et al., 2010). There is a growing body of literature that use long time series of fine spatial resolution images for the analysis of fire histories in annual approaches to different global landscapes, such as for savanna areas of South Africa and Botswana (Hudak and Brockett, 2004), arid grasslands of Australia (Greenville et al., 2009), Mediterranean grasslands of Spain (Röder et al., 2008), rainforest of Amazon (Alencar et al., 2011; Morton et al., 2011) and in the core areas of the Cerrado (Daldegan et al., 2014; Lemes et al., 2014).

It is worth noting that unlike countries such as Canada, with the Canadian Wildland Fire Information System (CWFIS) (CFS, 2017), United States, with the Monitoring Trends in Burn Severity (MTBS) Fire Occurrence Dataset (USGS and USDA, 2017), and Spain, with the Spanish Department of Defense Against Forest Fires Stats database (ADCIF, 2017), which contain systematic record of decades of valuable information, Brazil does not have database of fire occurrences with similar characteristics. Fire Incident Report (ROI, Portuguese acronym) is the official database, available from the National Forest Fires Prevention and Combat System (PREVFOGO), linked to the Brazilian Institute of the Environment and Renewable Natural Resources (IBAMA). Most of ROI data lack temporal and spatial continuity and are related to fire occurrences in protected areas where actions for their extinction were employed. Although efforts have been made to develop burned area detection algorithms adapted to fire behavior in Brazilian biomes (Libonati et al., 2015; Melchiori et al., 2014; Shimabukuro et al., 2015), an official spatial database that accounts for fire-affected areas is not yet available. The most relevant current achievement is presented by the Burning Monitoring Program of the National Institute for Space Research (INPE), through the 'Queimadas project' (INPE, 2017), which is introducing initial results of an automatic algorithm of burned areas detection at 30 m spatial resolution (known as AQ30m), restricted to the core area of the Brazilian Cerrado biome for the period of 2011 to 2015.

Pending availability of improved outcome results, the estimation of burned areas on local and regional scales, especially in the protected areas of the Brazilian National System of Conservation Units (SNUC), nowadays is based on accumulated active fire data derived from sensors of moderate/low spatial resolution. Although this information has been very relevant in the development of fire alert systems in areas of difficult accessibility, they present many limitations due to their direct interpretation as burned areas (Schroeder et al., 2010). Furthermore, validation of the major currently available global burned area products present high omission errors (Libonati et al., 2014; Padilla et al., 2015), which is not compatible with the generation of fire recurrence databases at local/regional scales.

Among different sensors applied in the burned areas assessment and monitoring, it is possible to highlight those that are aboard the series of Landsat satellites (Thematic Mapper - TM, Enhanced Thematic Mapper - ETM+, Operational Land Imager - OLI), Terra and Aqua (Moderate Resolution Imaging Spectroradiometer - MODIS). More precise and quite acceptable information for land management at local/regional scale is derived from the Landsat series (Lentile et al., 2006), which currently has more than four decades of global coverage. On the other hand, the MODIS series offers daily information, in a lower spatial resolution, allowing a more exhaustive temporal monitoring from 2000 to the present day (Giglio et al., 2013).

High temporal resolution information on burned area is needed to improve analysis of the fire affected areas in tropical savannas. Fires occurring before or at the beginning of dry season are generally cooler and less intense, while those occurring in the months of accumulated and dry fuel loads (usually the central and late months of the dry season)

burn intensely (Andersen et al., 2005; Williams et al., 1998). Higher damage to woody vegetation is related to this period of intense fires, more susceptible to the spread beyond tree vegetation formations (Laris et al., 2016; Nepstad et al., 2004). Furthermore, in some years the influence of climatic anomalies in the Amazon, such as regional climate phenomena El Niño Southern Oscillation (ENSO) and the Atlantic Multidecadal Oscillation (AMO), are present (Lewis et al., 2011; Marengo et al., 2011, 2008). They are usually associated with severe droughts, variations in precipitation regimes, temperatures and evapotranspiration levels.

Unlike the large literature regarding fire histories in annual approaches, few studies have investigated the seasonality of fire incidence using fine spatial resolution time series. To date, researches with these characteristics are restricted to selected areas of the Australian (Russel-Smith et al., 1997) and African (Laris, 2002, 2005) savannas. Yearly/seasonally studies based on coarse resolution time series are more recurrent, such as those of the Mediterranean vegetation in Israel (Levin and Heimowitz, 2012) and the savanna-forest contact areas in Madagascar (Jacquin and Goulard, 2013). For the Cerrado and the Amazon areas, available seasonal studies are based mainly on the analysis of satellite active fire information (Alencar et al., 2015; Chen et al., 2013; Schroeder et al., 2009). Although accumulated active fire points enable key moments related to the annual/seasonal incidence of fire to be estimated and provide relevant information in studies on a coarse scale, they restrict the direct interpretation to a total of burned areas and number of fires (Schroeder et al., 2008). The coarse spatial resolution of these products and the high omission rates, especially in relation to small fires (Laris, 2005; Schroeder et al., 2010), limit their use to a regional/local analysis of this phenomenon.

This lack of seasonal studies of fine spatial resolution is mainly related to the constraints imposed by the influence of atmospheric perturbations combined with a reduced temporal resolution of the Landsat series, which limit the interpretation of its date of burning and consequently its seasonal assignment (Laris, 2005). In this view, different researches have explored the potential of combining fine and coarse spatial resolution temporal series (i.e. Landsat and MODIS) to address problems of availability of fine resolution multitemporal records, such as in the study of spatio-temporal patterns of forest changes in Guatemala (Hayes and Cohen, 2007), in the estimation of spatial and temporal patterns of aboveground biomass of sandy grasslands in China (Yan et al., 2015) or in the multi seasonal mapping of land cover over complex Mediterranean environments in Portugal (Senf et al., 2015). Regarding topics more specifically associated with fire dynamics, recent studies have demonstrated the potential of the MODIS series for accurate time information on burned areas (Boschetti et al., 2015; Panisset et al., 2014; Veraverbeke et al., 2014).

In this context, this work aims to explore the combination of multiple remote sensing data sources - Landsat and MODIS surface reflectance, Tropical Rainfall Measuring Mission (TRMM) pluviometry and Vegetation Continuous Field (VCF) tree cover layers - to analyze spatial and temporal patterns of fire incidence in one of the biggest enclaves of savanna vegetation in the southern Brazilian Amazon, the Campos Amazônicos Savanna Enclave (CASE). The analysis is based on all the coincident time series of Landsat and MODIS available until now (2000–2016), seeking to: i) generate an annually/seasonally fire database of fine spatial resolution (30 m) for the last 17 years; ii) assess the relationships between seasonality and the extent and frequency of fires; iii) analyze the connections between fire seasonality/recurrence and the woody cover areas affected by fire.

This is the first study that generates and analyzes an annual/seasonal database of fine spatial resolution on the incidence of fire on South American savanna environments. At the same time, it presents an original methodology that combines remote sensing data sources to monitor and assess spatial and temporal incidence of fire, providing an important opportunity to advance over the restricted literature that deals with the seasonal study of fire in fine spatial resolution. Thus,

this study contributes to the understanding of fire dynamics and its repercussions on total environment, generating valuable data in the field of fire management on a local/regional scale.

2. Materials and methods

2.1. Study area

The CASE (Fig. 1) has a total area of 4342 km², located in the south-western quadrant of the Brazilian Amazon, covered by the municipalities of Manicoré, Humaitá, Novo Aripuanã (State of Amazonas) and Machadinho D'Oeste (State of Rondônia). Currently, the CASE is almost entirely integrated as a protected area within SNUC, with 47% belonging to the limits of the Campos Amazônicos National Park (CANP), 46% in the Tenharim Marmelos Indigenous Land (Marmelos IL) and 5% in the Tenharim Igarapé Preto Indigenous Land (Igarapé Preto IL) (Fig. 1c).

The climatic conditions of the region are characterized by high annual average temperatures, ranging between 24 °C and 28 °C, and an annual rainfall of up to 2000 mm. The period from November to March is considered wet season, while dry season extends from May to September; the months of April and October usually correspond to the transition between the two seasons (Marengo et al., 2001). Fire activity tended to increase exponentially with the decrease of rainfall in the dry season (Aragão et al., 2008). From a geological point of view, the area is part of Central Brazil Shield (southern Amazonian Craton) and the main geological formation is derived from the Neoproterozoic (*palmeiral* formation), a sedimentary lithology. In general terms, the topography is composed predominantly by flat slopes and dystrophic soils (neosols marked by the presence of *plinthite* in the B horizon), with soil type variations associated mainly in areas of riparian vegetation (Motta et al., 2002; ICMBio, 2016).

CASE is a continuous area of predominance of savanna phytophysiognomies in a region dominated by rainforest vegetation (Fig. 1a) and is considered one of the biggest savanna enclaves in southern Brazilian Amazon. The group of vegetation formations of the CASE region is classified as disjunct Amazonian savannas (Ratter et al., 2003), which corroborates the possibility that, in addition to the modern environmental factors, the current vegetation pattern of the area reflects the dynamics of the climatic changes of the Tertiary and Quaternary periods (Carneiro Filho, 1993). It is possible that in this area of relict vegetation isolated from the core of the Cerrado biome, speciation processes are in progress, making its protection extremely important for conservation of genetic biodiversity (ICMBio, 2016).

Vegetation formations of Cerrado (*sensu lato*) are not restricted to savanna formations, including variations ranging from grasslands to forests. Among herbaceous areas are the grassland without shrubs or trees (*campo limpo*) and grassland with scattered shrubs and small trees (*campo sujo*). The savanna formations are divided in: *campo cerrado* - scattered trees and shrubs and a large proportion of grassland; and *cerrado (sensu stricto)* - dominated by trees and shrubs (often 3–8 m tall), but with still a considerable amount of herbaceous vegetation. The next stage is a forest formation named *cerradão*, an almost closed woodland with crown cover of 50% to 90%, often of 8–12 m or even taller. Forest formations also include riverine forest (riparian vegetation) (Oliveira-Filho and Ratter, 2002). Geomorphological processes related to soil fertility, water dynamics and fire recurrence are elements that play an important role in the dynamics of these vegetation formations (Dantas et al., 2013; Miranda et al., 2009).

The proportion of tree cover is an important criterion for distinguishing these phytophysiognomies (Fig. 1b). Within the CASE, areas with a low percentage of tree cover (tree cover < 15% of the pixel) predominate, with a total area of 46.19%, closely linked to the predominant areas of grassland formations. The areas with predominance of high tree cover (tree cover pixel superior to 50%) total 19.75% of the enclave, while the rest of the area is occupied by the transitional classes, in which areas of savanna formations are linked to grassland or tree

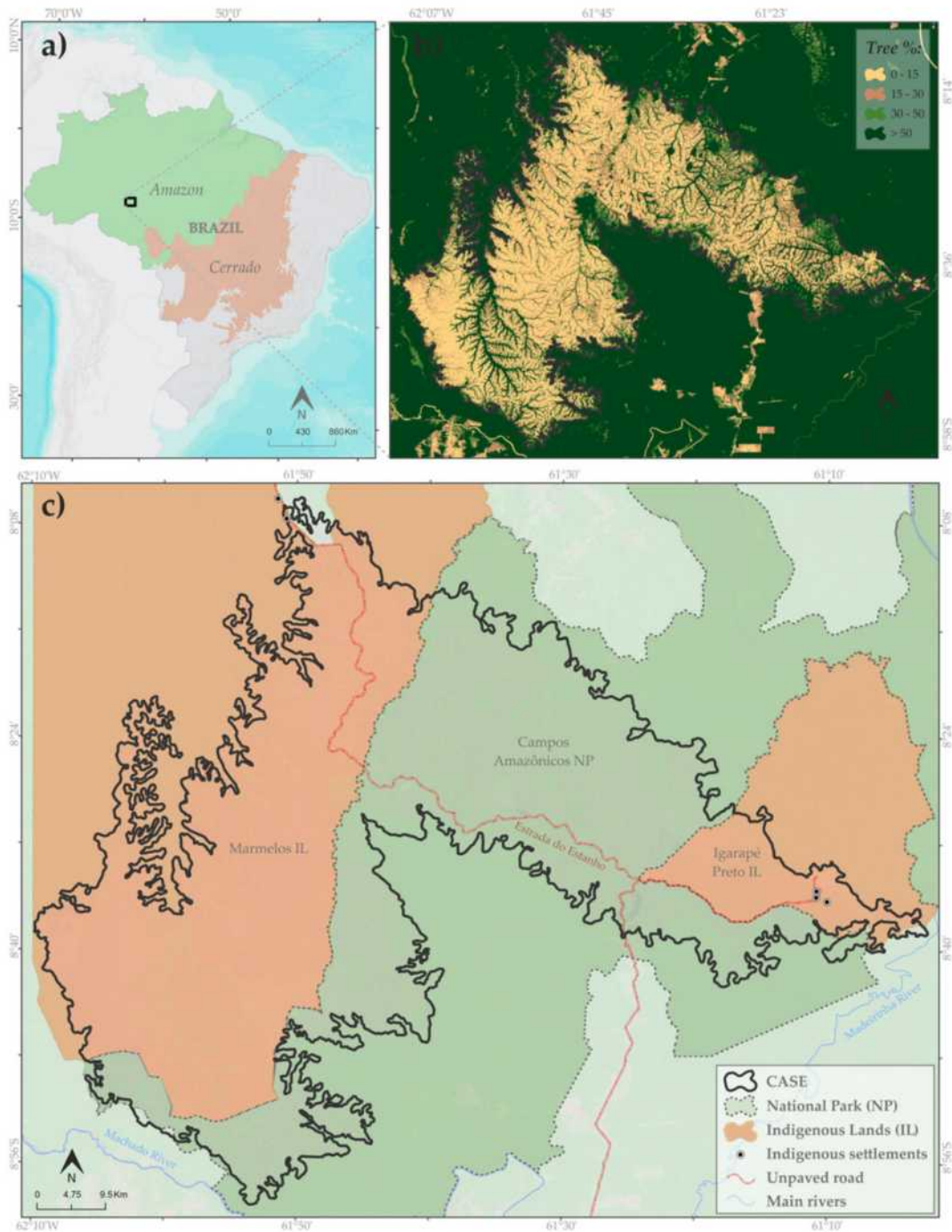


Fig. 1. Map of the study area: a) the CASE in the middle of the area of predominance of Amazon biome; b) tree cover (% per pixel); c) CASE almost totally integrated to areas of the CANP and Marmelos and Igarapé Preto IL.

formations. Grassland and savanna formations predominate in the interfluvial areas of the existent high drainage density network, while forest formations are mainly located in the proximity of the fluvial courses. Forest formations also appear in the form of more extensive fragments either in the border areas of the enclave (typical rainforest transitional vegetation) or in savanna forested areas (*cerradão*) (ICMBio, 2016).

The demographic density within the CASE is estimated at 0.10 inhab/km², the population is mainly concentrated in small indigenous settlements (Fig. 1c). During 1990s and at the beginning of the 2000s, areas located near the Estanço Unpaved Road, now belonging to the CANP, were used for agro-pastoral activities by approximately

50 families (ICMBio, 2016). At the time of creation, in 2006, the limits of the CANP did not include the areas within the distance of 10 km from the Estanço Road. These areas have been officially integrated into this conservation unit in 2012. The monitoring operations coordinated by IBAMA and the Chico Mendes Institute for Biodiversity Conservation (ICMBio), after the creation of the CANP, resulted in notable advances in the control of the illegal occupation of public lands in the region. As a result, agro-pastoral activities are currently very restricted within the CASE, legally established with the purpose of conserving the natural heritage associated with the biodiversity of this important enclave of Cerrado (ICMBio, 2016).

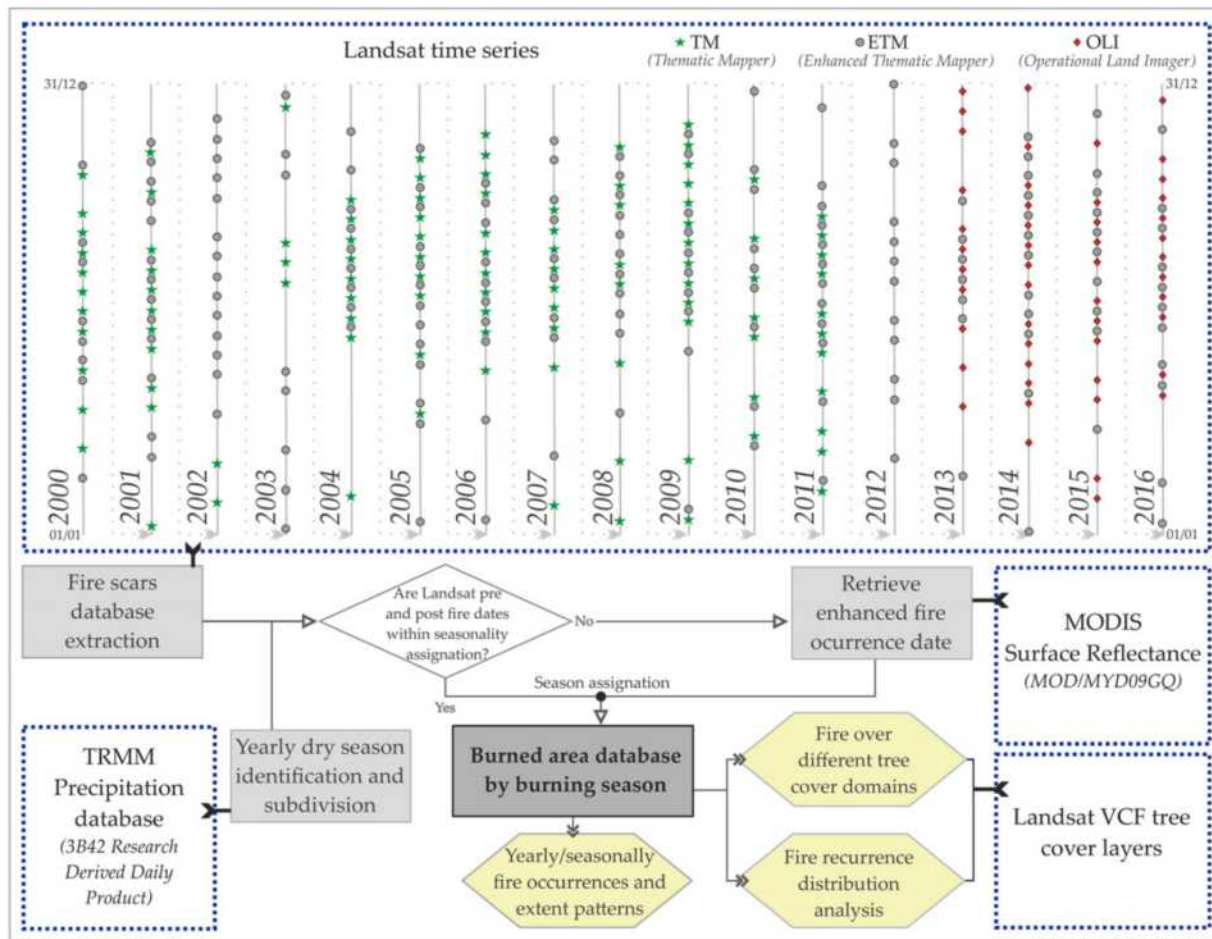


Fig. 2. Methodology workflow. Remote sensing data sources are shown with dotted boxes. Hexagons present layers resulting from analysis of the generated database.

2.2. Materials and methodological procedures

The methodological procedures (Fig. 2) follow four main steps: i) fire scars assessment; ii) dry season identification and subdivision; iii) retrieval of enhanced fire occurrence date; iv) assessment of temporal and spatial patterns of fire incidence. In the following subsections each step is described in more detail. Detailed information about the multiple remote sensing data sources used is available in Table 1.

2.2.1. Fire scars assessment

The Landsat TM, ETM + and OLI time series available for the period analyzed (2000–2016) are the main source for the identification of

burned areas. These sensors capture information from spectral regions relevant for analysis of vegetation dynamics, i.e. the Near Infra-Red (NIR), Short Wave Infra-Red (SWIR) and Red, with a spatial resolution of 30 m. Although the temporal resolution for each sensor is 16 days, there is a time overlap in operation of at least two sensors for almost the whole analyzed period, resulting in availability of Landsat records every 8 days. Exceptions correspond to the period between March 2002 and June 2003, when no TM images were acquired, and from November 2011 to February 2013, time period when the TM sensor stopped functioning and the images from OLI sensor has not been yet available.

A total of 334 images (dismissing those totally clouded) were downloaded from <http://earthexplorer.usgs.gov> (path/row – 231/

Table 1 Characteristics of the multiple remote sensing data sources used.

Remote sensing data source	Spatial resolution	Temporal resolution	Availability	Selected layers	Reference
Landsat TM Surface Reflectance	30 m	16 days	July 1982–May 2012	RED, NIR and SWIR (bands 3, 4 and 7)	USGS, 2016a
Landsat ETM + Surface Reflectance	30 m	16 days	April 1999–present	RED, NIR and SWIR bands (bands 3, 4 and 7)	USGS, 2016a
Landsat OLI Surface Reflectance	30 m	16 days	Feb. 2013–present	RED, NIR and SWIR bands (bands 4, 5 and 7)	USGS, 2016b
MOD09GQ - Surface Reflectance - V6	250 m	Daily	Feb. 2000–present	RED and NIR bands	Vermote and Wolfe, 2015a
MYD09GQ - Surface Reflectance - V6	250 m	Daily	July 2002–present	RED and NIR bands	Vermote and Wolfe, 2015b
TRMM 3B42 Research Derived - V7	0.25°	Daily	Jan. 1998–present	Total precipitation layer	Huffman et al., 2007
Vegetation Continuous Field tree cover layer	30 m	5 years	2000, 2005, 2010, 2015	Tree cover percentage layer	Sexton et al., 2013

66). It is worth mentioning that the greatest extensions in the study area are burned during the dry season, the period of greater availability of cloud-free Landsat acquisitions registered in the South of Brazilian Amazon (Asner, 2001) and in the core areas of the Cerrado (Sano et al., 2007). The rest of the year is characterized by high levels of precipitation, lower frequency of fire occurrences, and fewer high quality satellite images (Aragão et al., 2008).

The pre-processing started with the check of the root mean square error (RMSE) values related to the geometric model of the images. The images with RMSE >0.2 pixels (28 images) were co-registered using Global Land Survey (GLS) data as reference (USGS and NASA, 2010) to ensure geometric quality of the data. Landsat Ecosystem Disturbance Adaptive Processing System (LEDAPS) was applied for atmospheric correction of Landsat TM and ETM+ images (reflective bands) (USGS, 2016a). This algorithm employs a MODIS/6S radiative transfer approach (Masek et al., 2006; Vermote et al., 1997) taking into account ancillary water vapor data from NCEP (National Centers for Environmental Prediction) and TOMS (Total Ozone Mapping Spectrometer) data, with aerosols obtained from the image itself using the dark dense vegetation methodology (Kaufman et al., 1997). For OLI images, Landsat 8 Surface Reflectance Code (LaSRC) algorithm uses the scene center for the sun angle calculation and then hardcodes the view zenith angle to 0. The solar zenith and view zenith angles were used for calculations as part of the atmospheric correction (USGS, 2016b). LEDAPS and LaSRC codes are freely available from Center Science Processing Architecture (ESPA) of the United States Geological Survey (USGS) Earth Resources Observation and Science (EROS) members. 'Nodata' masks were applied to areas identified as clouds, high aerosol effects, shadows and areas affected by failure of Scan Line Corrector (SLC) on Landsat ETM+ after March 2003.

The extraction of the burned areas was based on an exhaustive process of visual interpretation, considering the chronological sequence of available images. Visual interpretation of fire incidence is a technique traditionally used in detection of burned areas. Although quite time-consuming, the process is considered relatively simple and allows obtaining reliable results (Bastarrika et al., 2011). It is generally used to generate validation data to assess accuracy of burned area algorithms (Bastarrika et al., 2014; Fraser et al., 2000; Melchiori et al., 2014).

Automatic and semi-automatic methods for extraction of burned areas proposed in the literature (Bastarrika et al., 2014; Melchiori et al., 2014; Shimabukuro et al., 2015) generally require complementation with visual interpretation to overcome commission and omission errors (Daldegan et al., 2014), which can occur due to the complex spectral and spatial heterogeneity of fire scars (Pereira, 2003). In an evaluation of different methods for extraction of burned areas in a tropical savanna region using Landsat images, visual interpretation allowed obtaining results similar and better to those obtained with the use of automatic and semi-automatic methods (Bowman et al., 2003). An example of a burned areas database essentially based on visual interpretation of Landsat images is the National MTBS Fire Occurrence Dataset (Eidenshink et al., 2007; USGS and USDA, 2017). Another relevant database based on visual interpretation is the cartography of forest fires of Portugal (ICNF, 2017).

Differenced Normalized Burn Ratio (dNBR) (Eq. 1) was used to assist the visual interpretation process. This index relating NIR and SWIR bands from the pre- and post-fire images is widely used to discriminate burned from unburned areas and estimate vegetation burn severity classes (Key and Benson, 2006). As a result of this step, fire scars were obtained for the entire time series analyzed, always accompanied by their temporal information available from Landsat (dates before and after fire).

$$dNBR = \frac{(NIR + SWIR)_{NBRpre}}{(NIR - SWIR)_{NBRpre}} - \frac{(NIR + SWIR)_{NBRpost}}{(NIR - SWIR)_{NBRpost}} \quad (1)$$

2.2.2. Dry season identification and burning periods subdivision

For an adequate comparison of burned areas by periods, the transition between the different seasons that affect the study area needs to be correctly defined. In the CASE region, double error can occur stating that in each analyzed year the dry season begins at the end of April and ends at the beginning of October. The beginning and end dates of the dry season vary from one year to another. When the intra-monthly variations of rainfall values are disregarded, it is possible to assign a fire occurrence to a wet season instead of dry season, giving way to one omission and other commission error, simultaneously.

To overcome these errors, the radar-derived rainfall data of TRMM were used to define and subdivide dry season in each analyzed year. More specifically, the data derived from the 3B42 Research Derived Daily Product (available at <<https://pmm.nasa.gov/data-access/downloads/trmm>>) were used. The product provides daily precipitation information for latitudes between 50° N-S, from 1998 to present, with a spatial resolution of 0.25° × 0.25°. This product is currently produced based on version 7 of the TRMM Multisatellite Precipitation Analysis (TMPA) (Huffman et al., 2007), that provides a calibration-based sequential scheme for combining precipitation estimates from multiple satellites.

The rainfall data were separated annually, initially identifying the dry season of each year. To achieve this goal, binary segmentation method (Binseg) was applied. The method assessing the mean and variance values of the data is available with the 'changeoint' package (Killick and Eckley, 2013) implemented in CRAN R software (RCT, 2016). The application is based on the fact that the transitions from wet to dry seasons are marked by a relatively rapid increase/decrease of the rainfall values (~4–5 mm/day) (Fu et al., 2013). Considering local climatic characteristics, the beginning of dry season was identified for each year from the rainfall data for the months of March, April (usually identified as a transition month) and May, forcing the identification of two segments that indicate the transition date. The same process was carried out with data from September, October and November to identify the transition that marks the return of the out-of-dry season.

Within each dry season, three burning periods were identified: early dry season, middle dry season and late dry season. This division seeks to overcome the problems associated with a dual division (early and late) in fire studies of savanna environments (Laris et al., 2016). The annual demarcation of these three periods was controlled by the definition of the middle dry period. Areas burned in the early dry season are those corresponding to the fires occurred between the beginning of the dry season and the beginning of the middle dry period, while the late burned areas are defined by end of the middle period and the end of the dry season. The middle period (locally named as 'modal' period) is defined as being the one that registers the longest uninterrupted period with minimum level of rain during the dry season, usually occurring between the second half of July and the first half of September. In the studied region, its beginning is associated with a small rainfall peak in July (not present in all years), which defines the entry of a more intense drought of approximately 50 days.

For the delimitation of the middle dry season, the longest continuous period with daily rainfall <5 mm recorded was identified in each dry season. In years with small rainfall peak in July (10 of the 17 analyzed years), the establishment of this initial criterion allowed automatic definition of the period. For the remaining years, the initial criterion allowed the correct extraction of the final date of each middle dry period. The initial date was then recalculated considering the average time elapsed between the initial dry season and the beginning of the middle period of the other ten years, added to the initial date of the dry season of those years.

2.2.3. Retrieval of enhanced fire occurrence date using daily MODIS database

In order to obtain a more precise date for the fire scars, surface reflectance images of version 6 of the products MOD09GQ and

MYD09GQ (Vermote and Wolfe, 2015a, 2015b) derived from the MODIS sensor on board Terra and Aqua satellites, respectively, available at <<https://e4ftl01.cr.usgs.gov/>> were used. The pre-processing of these products began with the download and creating mosaic (horizontal/vertical - 11,12/09) for the entire time series analyzed, ending with the association of 'no data' for pixels that did not present values considered acceptable in the quality flag bands (excluding pixels with cloud, cloud shadow or high aerosol effects identified). Although these products have a lower spatial resolution than Landsat (250 m × 30 m), higher temporal resolution of MODIS, with a global daily revisit of each of its satellites, increases the accuracy of the estimated date of the fire scars. Fire affected areas are visible thanks to the daily variations of the reflectance values in the Red and NIR bands (Trigg and Flasse, 2000).

For correct season/subseason assignment of each burn this check was performed for 496 fire scars that could not be classified based on the temporal information obtained with Landsat. When the fire occurred on the transition days between the seasons (23 fire scars), the evolution of the scar between the dates was considered. In this case the highest amount of burned area over a given season was used as discretization criterion. Limitations related with the lower spatial resolution of MODIS were visible in a total of 38 fire scars (burned areas < 8 ha - approximately 1 pixel MODIS). In these cases, the decision was based on visual interpretation of the post-fire Landsat image, since it was possible to infer that burns which appear closer to the post-date image usually present a stronger scar signal than the burned areas which occurred more distant from the date. It should be noted that these specific cases represent only 4.26% of the number of fire occurrences.

2.2.4. Assessment of temporal and spatial patterns of fire incidence

Stratification and analysis of the fire incidence statistics was carried out using database obtained in the previous steps. It is based on the yearly and seasonal data, which include the total number of occurrences, the total area, the average area, the median and the standard deviation. Each fire scar was also categorized according to its size in very small (>15 ha), small (15–100 ha), medium (100–1000 ha), large (1000–5000 ha) and very large (>5000 ha). These metrics, traditionally applied in landscape ecology studies of vegetation fragmentation, are quite useful in interpreting fire incidence. They allow characterization and detection of spatial patterns, being commonly used for analysis of

the fire-affected areas (Alencar et al., 2015; Daldegan et al., 2014; Moreno et al., 2014).

The 'yarr' R package (Phillips, 2017) was used to explore the seasonal patterns of the burned areas distribution by size. This package makes it possible to generate graphical sample distribution information that (i) allows representation of the whole data set; (ii) explains central tendency and density of data distribution, i.e. bean smoothed density (Kampstra, 2008); and (iii) allows the statistical inference from the data, employing Bayesian Estimation Supersedes the T-Test (BEST) (Kruschke, 2012) to generate 95% Highest Density Intervals (HDI) for the mean of each group.

In addition, the Landsat VCF tree cover layers provided by the Department of Geographical Sciences of the University of Maryland and NASA, were used to identify the areas of the highest fire frequency. This product results from rescaling 250-m MODIS VCF Tree Cover dataset using Landsat images and ancillary data; Laser Imaging Detection and Ranging (LIDAR) data being used as a reference for assessment of product accuracy (Sexton et al., 2013). Data available for each 30 m pixel were classified in four tree cover domain categories: low (0–15%); medium-low (15–30%); medium-high (30–50%); and high (>50%). Considering the time resolution of the product, currently available for the years 2000, 2005, 2010 and 2015, the closest available year was used to account for the affected areas annually. In other words, for the 2000–2004 period the product of tree cover 2000 was used, followed by the use of the base of 2005 for the years 2005–2009, tree cover 2010 for the interval from 2010 to 2014 and tree cover 2015 for the final two years of the series.

One-way analysis of variance (ANOVA) was applied to test for significant differences ($p < 0.05$) in two cases: (i) to compare the amount of fire affected areas of woody cover in different classes of burning periods; (ii) to check woody cover losses between 2015 and 2000 in different classes of fire recurrences areas. In both cases, the data were log-transformed to correct for heteroscedasticity and non-normality. Homoscedasticity was checked with the Levene's test ($p > 0.05$) and normality was assessed with the Kolmogorov-Smirnov test ($p > 0.05$). Post-hoc Tukey test ($p < 0.05$) was carried out to verify the significant difference levels in each independent class. Regression analysis was also performed to analyze the relationships between the total of burned areas and their respective subtotals in each tree cover domain classes.

Finally, the spatial distribution of the fire recurrence was analyzed based on the algebra of annual maps. High recurrence areas were highlighted over the final recurrence map to assist the interpretation

Table 2
Burned areas and number of fires by size categories. Years in which >20% of the CASE were burned are in bold.

Year	Number of fires (N) by size categories					N total	Total area (ha)	S (%) ^a
	<15 ha (very small)	15–100 ha (small)	100–1000 ha (medium)	1000–5000 ha (large)	>5000 ha (very large)			
2000	57	37	19	1	0	114	9720.00	2.24
2001	51	58	29	2	0	140	14,048.46	3.24
2002	62	36	31	8	1	138	30,378.69	7.00
2003	41	71	30	7	4	153	109,272.69	25.17
2004	74	77	33	5	1	190	31,996.62	7.37
2005	34	32	24	8	5	103	159,401.70	36.71
2006	34	26	17	4	3	84	66,709.26	15.36
2007	37	39	9	1	3	89	62,934.48	14.49
2008	11	11	5	1	1	29	79,072.92	18.21
2009	26	17	12	1	0	56	5761.53	1.33
2010	21	14	7	1	3	46	137,481.93	31.66
2011	18	1	0	1	5	25	95,479.47	21.99
2012	9	14	5	3	1	32	15,804.45	3.64
2013	26	11	5	0	0	42	2517.84	0.58
2014	41	23	10	4	2	80	145,089.00	33.41
2015	26	14	11	4	1	56	24,237.00	5.58
2016	25	16	8	3	3	55	38,548.98	8.88
Total	593	497	255	54	33	1432	1,028,455.02	236.86
Average	34.88	29.24	15.00	3.18	1.94	84.24	60,497.35	13.93
Sd	17.94	21.79	10.68	2.58	1.71	48.85	52,119.87	12.00

^a S (%) - relation between the total burned area and the total area of the CASE.

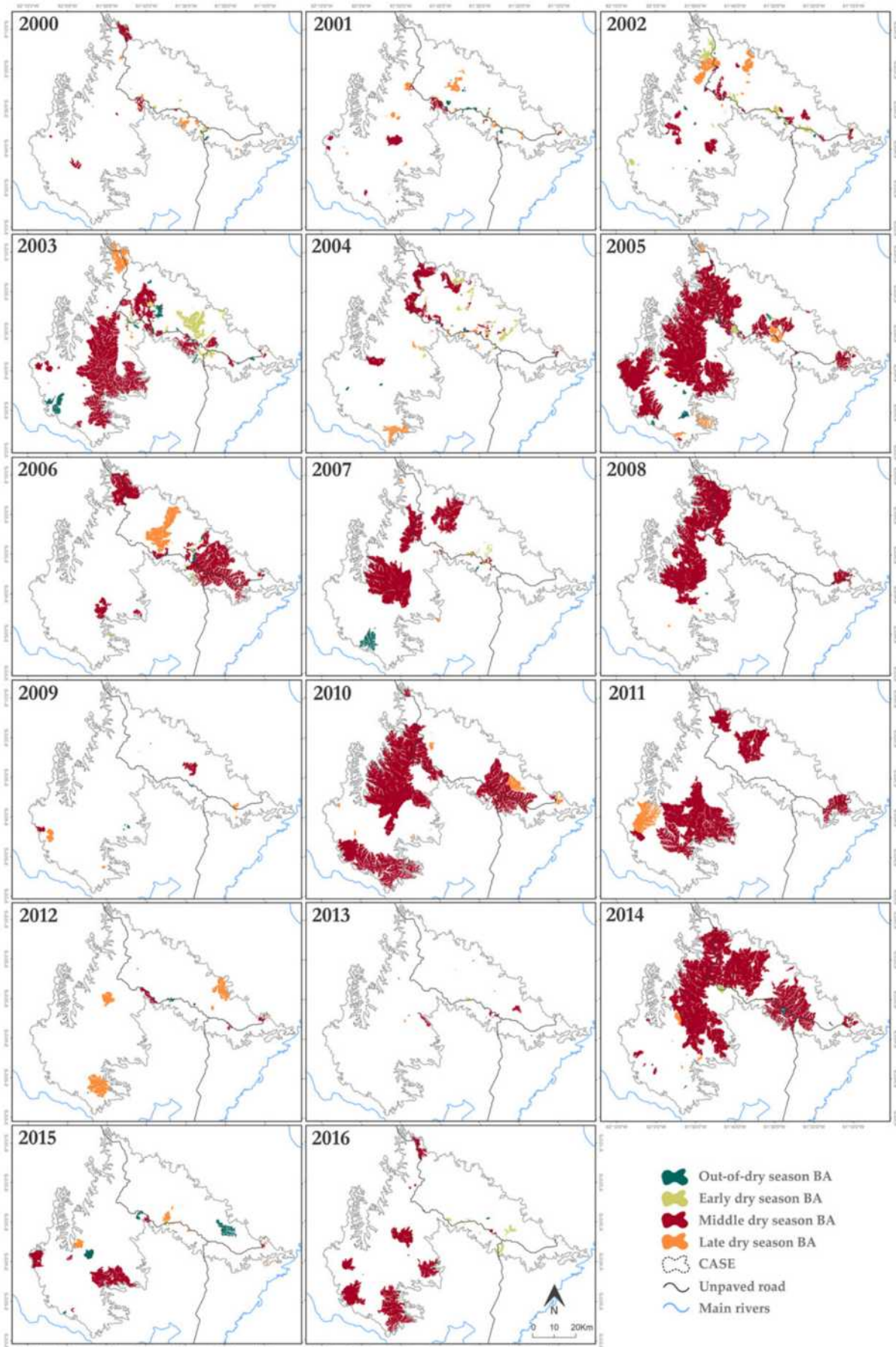


Fig. 3. Annual mapping of burned areas in the CASE between 2000 and 2016, divided by burning periods. White areas inside CASE delimitation represent unburned areas in the respective year.

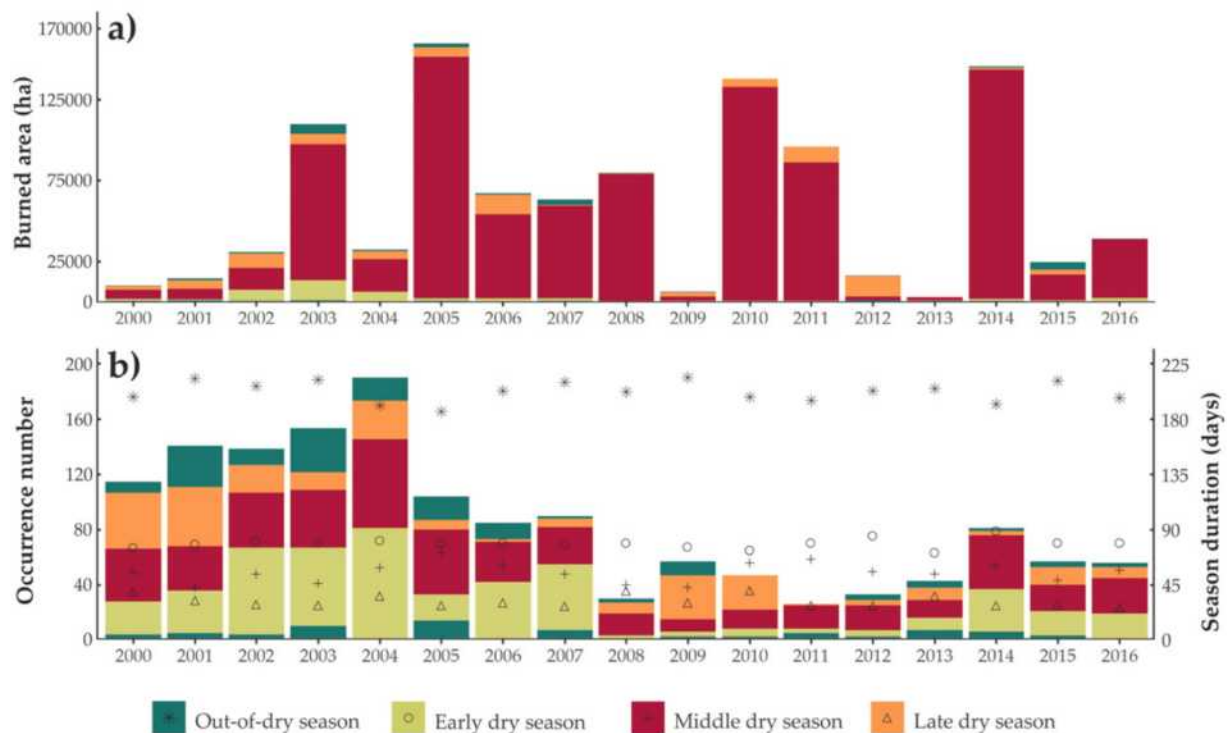


Fig. 4. Total of burned areas (a) and number of annual fire occurrences (b) in the CASE between 2000 and 2016, divided by burning periods. The out-of-dry season period is divided into two blocks, showing the proportion corresponding to before and after the annual dry season in the lower and upper parts of each bar, respectively. Dots mark the duration of the seasons.

of the areas more and less frequently burned, based on visual interpretation. Additionally, the tree cover products of 2000 and 2015 were used to contextualize this analysis.

3. Results

3.1. Yearly fire frequency and extent by size categories

In the last 17 years, a total of 1.03 million ha were burned within the CASE, distributed across 1432 fire occurrences (Table 2), corresponding to almost 2.5 times its total area, although about 30% did not record any fire in the series analyzed. The subtotals of the annual burned areas data highlight 2003, 2005, 2010 and 2014 as the years in which the totals were more than 100,000 ha, reaching the annual maximum in 2005, where 36.71% of the enclave was affected by the fire. In contrast, 2000, 2009 and 2013, with a maximum of less than 10,000 ha burned, are the least fire-affected years in the series, with the minimum being recorded in the year 2013 (2517.84 ha).

In relation to the size of the burns, it is notable that small and very small events predominate in relation to the other size categories. The number of fires in these categories, burning <100 ha, represents 76.12% of the total recorded for the whole period analyzed. However, these 1090 occurrences cover only 2.11% of the total areas burned for the period, contrasting with the 79.14% razed by 33 very large fires. The total area burned by very small, small and medium fires in the last 17 years (94,404 ha) is less than the 104,080 ha burned in the

largest fire in the time series, recorded in 2014. This data indicates how significant a very large fire can be in the CASE, an important aspect in relation to fire incidence in the area.

Also regarding the annual distribution of number of occurrences, it is noticeable that the initial years of the series were marked by a greater number of records in relation to the others, with 2004 as the year with the highest number of fires (190). This transition is marked by the years following 2004, where an abrupt decline is observed followed by relative stabilization of the number of events. The spatial representation of this process can be seen in more detail in the annual mapping of burned areas (Fig. 3). It is apparent that the vicinity of the Estanho Road was more heavily affected by fire in the early years of the series, such as 2001 and 2002, compared to years like 2012 and 2013, for example.

In addition to distinguishing burned or unburned areas, the annual mapping brings to the debate the seasonality of fire, an issue addressed in more detail in the following subsection.

3.2. Exploring fire seasonality patterns

The average annual dry season lasts for 163 days, with start and end dates between May 4 and October 14 on average (standard deviation of 6.70 and 6.76 days, respectively). In relation to the burning periods, the early dry season had the longest average duration (78 days), predominantly occupying the months of May, June and most of July each year. The end of the early period gives way to the middle dry season, which holds for approximately 54 days from July 20 to September 14. Between

Table 3
Number of fires aggregated by season and size categories.

Burning periods	Number of fires by size categories					Total
	<15 ha (very small)	15–100 ha (small)	100–1000 ha (medium)	1000–5000 ha (large)	>5000 ha (very large)	
Out-of-dry season	76	95	43	5	0	219
Early dry season	239	158	57	4	1	459
Middle dry season	168	161	100	35	27	491
Late dry season	110	83	55	10	5	263

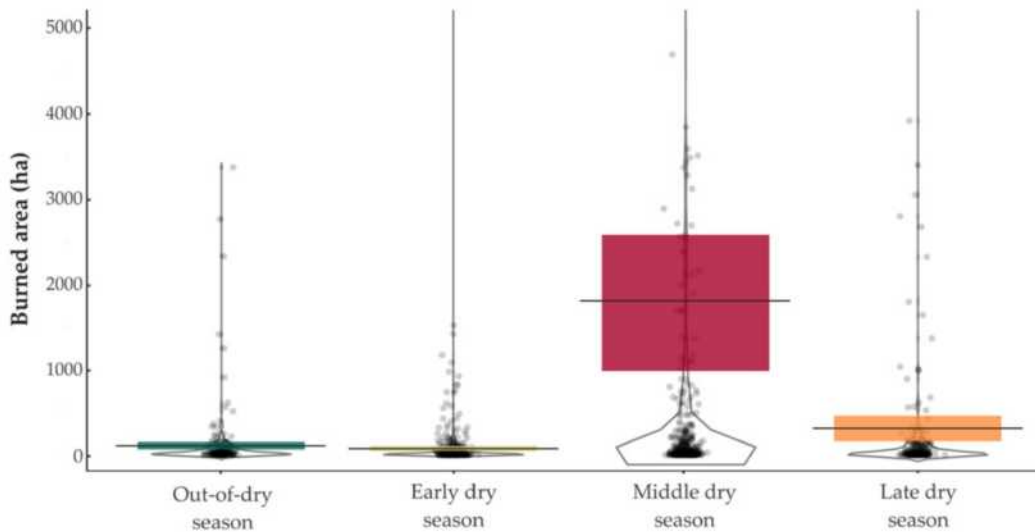


Fig. 5. Data distribution of all fires of up to 5000 ha (2000–2016) aggregated per burning seasons. Dots shows all row data (jittered horizontally) and indicate the size of each burn. Beans are linked with the smoothed densities of each burning season. The box represents the highest density intervals (95% HDI) and bar indicates central tendency (mean size) of each season.

the second two weeks of September and the 14th of October, the late dry season was observed, the shortest of the three burning periods (29 days on average). More detailed information on the annual burning periods can be seen in Appendix A.

Visualization of the annual maps reveals the relevance of the seasonal subdivision when interpreting the incidence of fire in the CASE. The maps highlight the dominance of burned areas occurring during the dry season, especially the middle period. Statistically, 97.64% of the total burned area is linked to the dry season, with a notable predominance of the middle dry season (86.21%), followed by the total burned area during the late dry season (7.98%). The number of fires is a more proportional datum, with totals of 491, 459 and 263 events for the middle, early and late dry seasons, respectively. Another 219 fire scars occurred in the out-of-dry season. These relationships are best explored by the graphical approach of the ratio of number of occurrences and total of burned area by burning seasons (Fig. 4).

The occurrences during the early dry season most resemble the out-of-dry season burnings, mainly in relation to the total area and the average size. It is noticeable that the largest number of fires in the early years of the series has repercussions mainly on those of the early and late dry seasons.

The years with the highest totals of burned area coincide with slight decreases in the duration of the out-of-dry season, as observed in the records of 2005, 2010 and 2014. However, the contrast between the out-

of-dry season duration and total burned areas registered in other years suggest that this relationship has not been established directly. Years such as 2000 or 2004, where there is a decrease in the out-of-dry season and relatively low total burned areas, and 2003, one of the years with a short dry season, while also recording one of the largest burned areas, are examples that relativize these statements. It suggests that the prolongation of the dry season, due mainly to prolongation of the middle dry season, can affect the record of high total annual figures of burned areas, although it is not a required condition.

A more detailed exploration of the relationship between size and season can be seen in the total of number of fires for each size category (Table 3) and in the aggregate of burned areas up to 5000 ha (Fig. 5).

The concentration of small and very small fires is a salient point in the bean smoothed density of all the burning periods. It is worth noting the less flattened bean densities in the distribution of late and middle dry season fires, especially in the latter. These differences mainly relate to the proportionally greater number of large and very large fires during these periods. More precisely, the middle period is where 81.82% of the very large fires are concentrated. During this period, the 16 largest occurrences of the temporal series were recorded, totaling 672,952 ha.

The highest density intervals (95% HDI) highlight the similar behavior of mean values of early and out-of-dry season fires (45.49 to 108.21 ha; and 62.96 to 155.64 ha, respectively). At the same time, the intervals of the middle dry season fires (between 1018.05 and

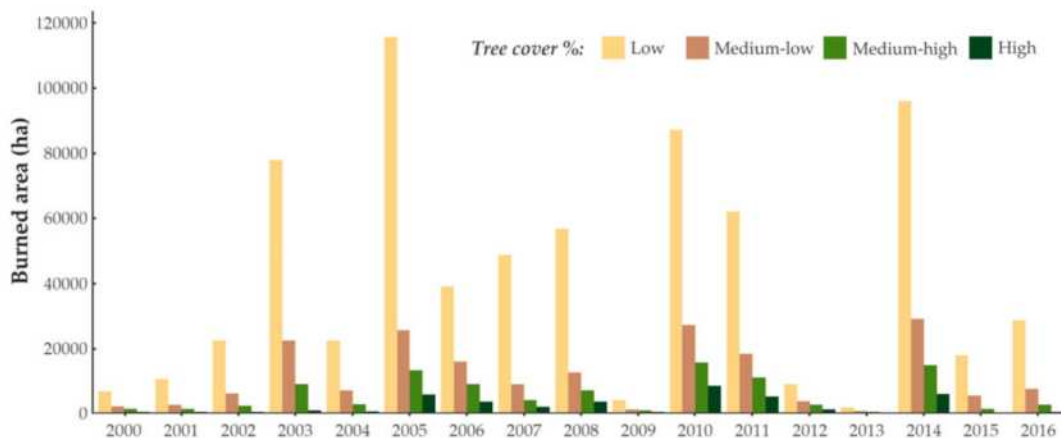


Fig. 6. Areas of different tree cover domain categories affected by fire annually.

Table 4
Subtotals of burned areas in different tree cover domains divided by season and size.

Season/size categories		Tree cover % domains							
		Low		Medium-low		Medium-high		High	
		ha	%	ha	%	ha	%	ha	%
Season	Out-of-dry season	17,146.08	70.57	4940.01	20.33	1799.91	7.41	409.50	1.69
	Early dry season	24,548.49	69.20	7604.82	21.44	2994.66	8.44	327.69	0.92
	Middle dry season	607,711.32	68.54	163,829.79	18.48	82,516.50	9.31	32,549.31	3.67
	Late dry season	53,650.80	65.37	16,580.43	20.20	8760.24	10.67	3080.97	3.75
Size	<100 ha	14,139.45	65.28	4344.84	20.06	2293.74	10.59	881.01	4.07
	100–1000 ha	47,379.24	65.13	15,722.46	21.61	7605.81	10.46	2032.65	2.79
	1000–5000 ha	79,219.80	65.92	26,288.82	21.88	11,673.54	9.71	2987.19	2.49
	>5000 ha	562,318.2	69.09	146,598.93	18.01	74,498.22	9.15	30,466.62	3.74

2583.58 ha) and late dry season fires (between 167.77 and 462.45 ha) do not overlaps with any other burning season 95% HDI. It makes possible to infer that fires in the middle dry season are bigger on average than those on other burning seasons. The same relation is verified between the late dry season fires compared to out-of-dry season and early dry season fires.

3.3. Fire patterns over different tree percentage cover domains

Areas of low and moderate/low tree cover domains were the most affected by fire categories in the whole time series, covering totals of 68.36% and 18.76%, respectively. On the other hand, a total of 132,439 ha of burned areas consisted of moderate/high and high tree cover domains, with totals of 9.34% and 3.54%. This hierarchy of proportions, associated with landscape configuration and the usual fire propagation behavior in the CASE, is observed in each year of the time series (Fig. 6).

The year 2010 registered 8286.57 ha burned from areas of high percentage of tree cover, the highest annual amount of areas burned in this type of domain, followed by 2014 and 2005. Although they do not follow the same order of ranking, these three years coincide with those most affected by fire in the time series.

The subtotals by burning periods and size categories (Table 4) show the areas with a high proportion of tree cover linking to the middle dry season (32,549.31 ha) and very large (30,466.62 ha) fire occurrences. Regarding seasonality, the proportional data show that, during the middle and late dry seasons, greater percentages of high tree cover domains are affected by fire (3.67% and 3.75%) compared to the early and late dry season burned areas (0.92% and 1.69%). Furthermore, very large and <100 ha events occurred in relatively greater proportions of high tree cover domains affected by fire.

Results derived from regression analysis (Fig. 7) explore in more detail the relationships between total burned areas and their respective subtotals burned in each tree cover domain category, taking the database as a whole. Although the coefficients of determination are more

adjusted in the relation between the total of burned areas with their subtotals in the categories low and medium-low tree cover domains (0.992 and 0.968, respectively), this relation continues strongly established in the categories of higher tree density (0.937 and 0.825 for medium high and high tree cover domains).

ANOVA test (Table 5) revealed significant differences ($F = 7512$; $p < 0.05$) between the proportion of medium/high and high tree cover domains areas affected by fire (related to their respective total area) compared by burning seasons categories, grouping all medium, large and very large fire occurrences. Results derived from Tukey's post-hoc test (Table 6) showed that during the middle dry season higher proportions of woody vegetation were affected by fire compared to early and out-of-dry season occurrences. However, these significant differences were not verified when comparing occurrences in the late dry season in relation to the other burning periods.

3.4. Spatial distribution of fire recurrence

The recurrence map of burned areas (Fig. 8) allows us to identify the constant presence of fire in the spatial dynamics of the enclave, with at least one burning recorded in 70.14% of the CASE within the series analyzed. Areas that have burned up to 4 times occupied 75.15% in relation to the areas that were burned at least once (Fig. 9a).

The overlapping of burned areas highlights the fragmented pattern of burning. The areas of riverine forests are usually associated with lower (or even non-existent) fire recurrence values. In contrast, interfluvial areas are usually the most frequently affected, as there is a predominance of vegetation formations with a low and medium low percentage of trees. Certain zones are more important in the spatial distribution of the areas of greatest recurrence.

The first is located in the south-western sector of the CASE (Zone A), an area predominantly belonging to Marmelos IL, where recurrence prevails over a large area, returning values >5 times higher (up to a maximum of 9 times). Zone B is also integrated with Marmelos IL, in the vicinity of the Estanho Road axis, where patches of high recurrence

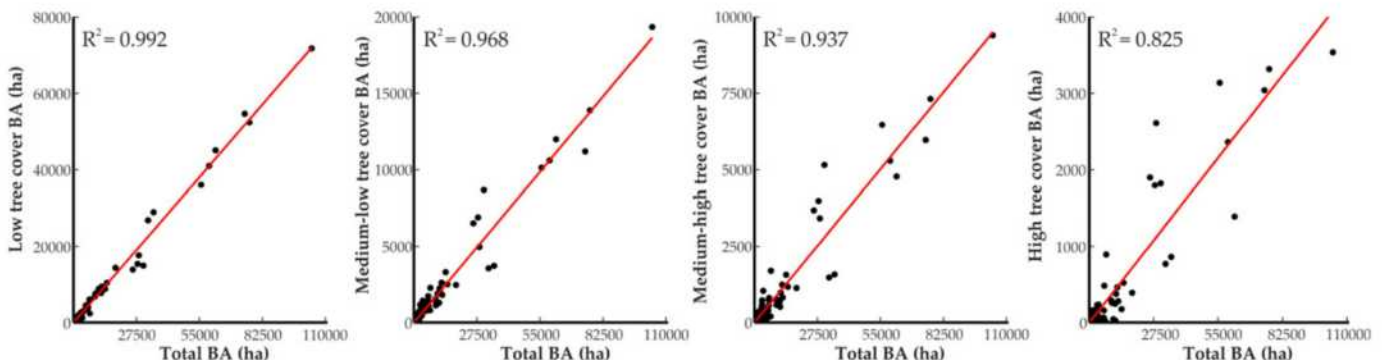


Fig. 7. Relation between total burned area (BA) and their respective subtotals by tree cover domain classes of all fires (2000–2016).

Table 5

Results derived from one-way ANOVA test - relations between burning seasons and proportion of woody cover fire affected areas (n = 342; all fires bigger than 100 ha).

	Degrees of freedom	Sum of squares	Mean square	F value	Pr (>F)
Between groups	3	19.197	6.399	7.512	0.0000891
Residuals	338	287.900	0.852		

Table 6

Tukey multiple comparisons of means - 95% family-wise confidence level.

Difference of levels		Difference of means	95% confidence interval	p-Value
Early dry season	Out-of-dry season	-0.130	(-0.588, 0.328)	0.883
Middle dry season	Out-of-dry season	0.460	(0.069, 0.852)	0.014
Late dry season	Out-of-dry season	0.206	(-0.241, 0.652)	0.634
Middle dry season	Early dry season	0.590	(0.235, 0.946)	0.000
Late dry season	Early dry season	0.336	(-0.080, 0.752)	0.159
Late dry season	Middle dry season	-0.254	(-0.595, 0.0864)	0.219

are generally more continuous and extensive, a pattern similar to that observed in Zone A. In contrast to these characteristics, Zones C and D present a spatial configuration of smaller patches, in areas largely belonging to the current limits of the CANP. These areas are adjacent to the Estanho Road and other small unpaved roads that were opened in the early years of the time series, now abandoned. Other small clusters can be seen around the Estanho Road with same characteristics as these two zones. The last area to be highlighted is Zone E, which is integrated into Igarapé Preto IL. In this area, small patches with high values of recurrence (reaching the maximum values of the series - 14 times) are observed.

An observation of the tree cover domain data from 2000 and 2015 (Fig. 9b), in association with each class of recurrence, repeats the

hierarchical pattern already observed in the annual, seasonal and by-size subtotals. As the number of recurrences increases, there is a progressive decrease in the proportions of high tree cover areas compared to low cover, reaching insignificant numbers in the class of 5 times burned. The comparison between values presented in tree cover in 2000 and 2015 suggests that more frequently fire affected areas are related to the loss of areas of medium/high and high tree cover domains. This can be clearly seen in the comparison of percentages of medium-high and high tree cover areas in the higher categories of recurrence (>3 times burned), which show losses contrasted with the relative stability verified in unburned areas. However, no significant differences were verified in the ANOVA tests (Table 7) between the highest proportion of affected woody vegetation and higher fire frequencies. The most

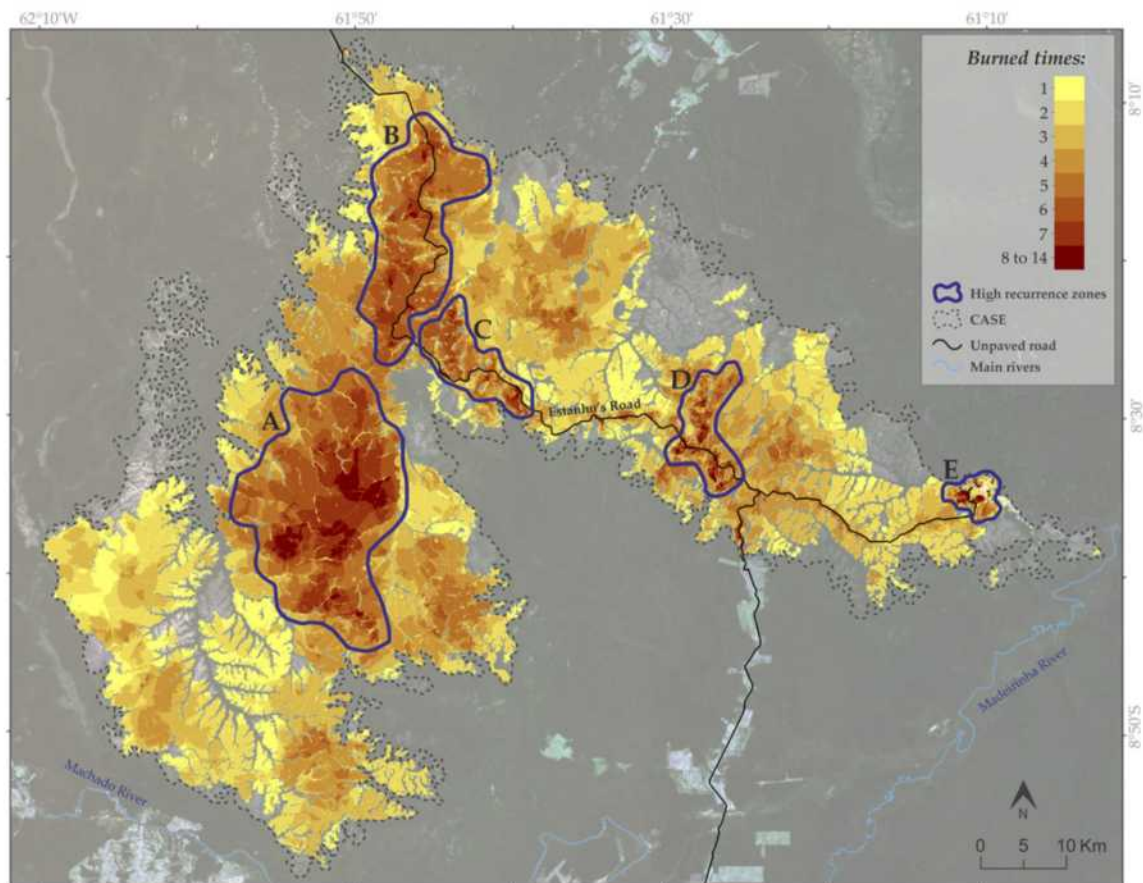


Fig. 8. Map of recurrence of burned areas in the CASE from 2000 to 2016. The background shows a Landsat-OLI image from July 27, 2016, composition in transparency (Green-Blue-NIR/R-G-B), which corresponds to unburned areas inside the CASE.

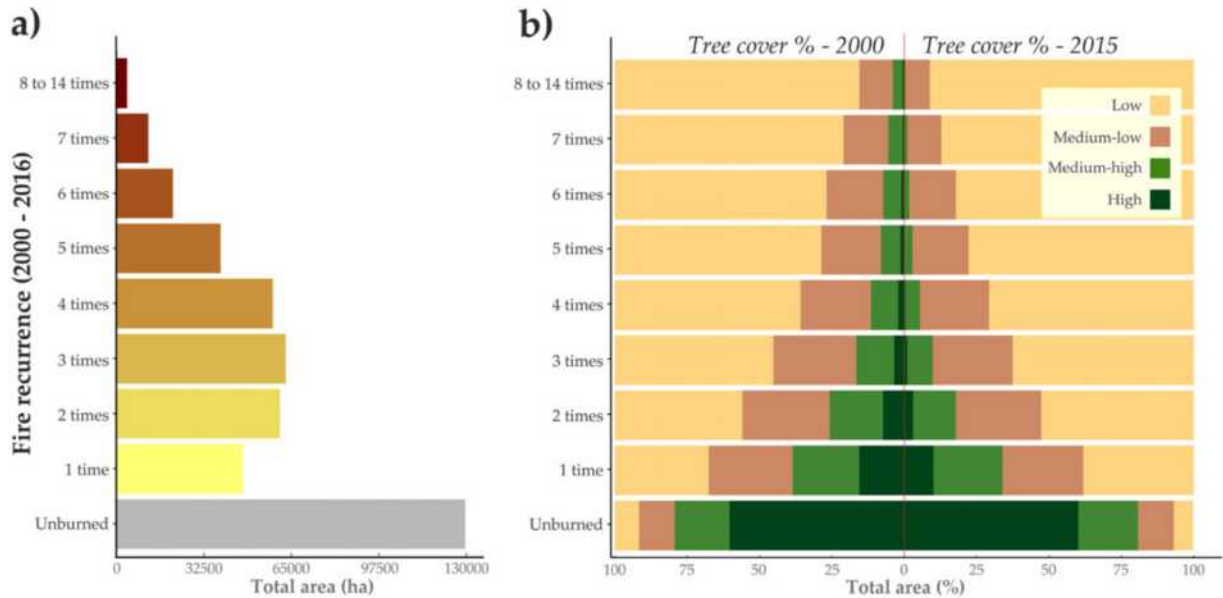


Fig. 9. Subtotals of the CASE fire recurrence map (a) and his respective percentages of tree cover domains in 2000 and 2015 (b).

Table 7

Results derived from one-way ANOVA test - relations between fire recurrence categories and losses of woody cover between 2000 and 2015.

	Degrees of freedom	Sum of squares	Mean square	F value	Pr (>F)
Between groups	7	2.390	0.341	0.734	0.643
Residuals	192	89.510	0.466		

abrupt differences observed in areas burned >9 times need to be weighted by the very low totals of burned areas of these category.

The unburned areas (29.85% of the enclave) include a large amount of riverine forests, mainly those that are more vigorous and extensive along the whole enclave. On the other hand, there are some patches of predominantly grass/savanna vegetation formations, the largest of them located in the central-eastern zone of the enclave, about 8 km north of the Estanho Road. Also in relation to tree predominance, areas of *cerradão* can be highlighted, such as the large area in the eastern zone of CASE (interior of Igarapé Preto IL), approximately 5 km north of the Estanho Road. In this area, the only fire of the series recorded nearby occurred as a late burn in 2010.

The subtotals of the unburned areas reveal that 60.14% occurred in high tree cover domain in 2015, followed by an also important percentage (20.62%) in medium-high tree cover. Medium-low and low tree cover domains represent 12.30% and 6.70%, respectively, and the remaining percentage (0.24%) belongs to river channels. The comparison of data for 2000 and 2015 shows that the predominance of these different categories remained relatively stable, with a slight increase in the medium/high tree cover areas in detriment to the low areas. It is worth noting this inversely proportional hierarchy of tree cover domain values between unburned areas and those that burned at least once.

4. Discussion

4.1. Yearly/seasonally fire occurrences and extent patterns

In the CASE, records of exceptionally large fires are found in common each year with high numbers of total burned areas, always linked to the middle dry season of their respective year. Yearly and seasonally analysis also reveals that the highest number of fires is not necessarily concentrated in the middle dry season, as they are often exceeded by the totals recorded in the late and/or early dry seasons annually. However,

potentially larger fires are clearly concentrated during this period, resulting in annual burned areas that are predominantly higher than the other burning seasons throughout the time series. As in the other tropical savannas, fires depend on two main factors: i) the type, condition and spatial (dis)continuity of the fuel loads in its zone of ignition and propagation; ii) the atmospheric conditions during propagation, especially the direction and speed of the wind and amount of rainfall. An ignition during the middle dry season, anthropogenic or natural, combined with adverse conditions associated with these factors (mainly with high spatial continuity of the fuel loads and the absence of rainfall) set the scenario for exceptionally large fires. Actions by fire brigades (increased since creation of the CANP) are very limited due to the great difficulties of access and lack of personnel, so natural extinction is the most common process.

In the conservation policies currently conducted by ICMBio in the CANP region, one of the main concerns is precisely the occurrence of very large fires. CASE is a large savannah area totally isolated from its core biome, and a fire that eventually reaches the whole area of the enclave could be catastrophic for its biodiversity (D'Amico, 2014). In a study of the impacts of fire on the megafauna of the Emas National Park, located in the core area of the Cerrado, the harmful effect of large fires for certain species is highlighted, especially damaging to individual giant anteaters (Silveira et al., 1999). Despite the documented fragility of some species, strategies linked only to fire suppression in Cerrado environments are inadequate, and may even instigate very large fires from excessive accumulation of fuel loads (Ramos-Neto and Pivello, 2000). In this perspective, preventive actions to limit the spatial continuity of fuel loads have been initiated by the CANP management team and its fire brigade in recent years, by constructing firebreaks and applying prescribed fires over strategic areas. The expansion of these preventive activities will depend on concrete advances with the fire management plan of the area, in which the database generated here and their respective analyses will be useful.

In the annual/seasonal dynamics of the number of fires in the CASE, the creation and consolidation of the current limits of the CANP coincides with the period of abrupt reduction in these values, followed by stabilization, linked to the notable advances in land regularization in the area. This process is clearly related to the abandonment of practically all of the agro-pastoral farms lying in the vicinity of the Estanho Road, where fire was frequently used for land preparation. More control established over the number of ignitions is a very important aspect for implementing a fire management plan, which is a positive influence of this protected area for the CASE. With the current territorial context of the area, together with increasing stabilization of the CANP and, consequently, greater monitoring capacity of anthropogenic ignitions, the tendency is for areas near the Estanho Road to remain stable, or even reduce the patterns of fire recurrence.

Two aspects regarding the spatial pattern of fires deserve to be highlighted, best seen in the large ones. The first aspect refers to the fragmented pattern of burning, inherent to tropical savannas, where the discontinuity of fire propagation is closely associated with the riverine forests and the other denser fragments of tree vegetation. There are many factors that can influence the extent to which the fire advances into the riverine forests, with some of the most important being the speed and direction of the wind and the condition of the fuel loads (humid or dry). The second aspect is that areas burned in the previous year often control or even delimit burning in the next year. This can be explained by the fact that the availability of fuel loads is limited by the previous year's burning damaging propagation.

Regarding the annual variability of total burned area, two of the three most burned years of the series (2005 and 2010) coincide with years of severe droughts in the Amazon (Lewis et al., 2011; Marengo et al., 2008). More specifically, they coincide with the years of greater positive oscillation of the AMO for the whole time series analyzed, with this climate anomaly more closely linked to fire activity in the southern and southwestern Amazon regions (Chen et al., 2011). These climatic anomalies were expressed in an increase in the duration of the drought periods of the analyzed series, mainly due to a prolongation of the middle period, generating conditions apparently more favorable to higher totals of annual burned areas. Although no regional climate anomaly was registered in 2014, the second most burned in the series, local rainfall data show similar conditions to the years 2005 and 2010, with a prolongation of the dry season.

However, other years in the series, such as 2000 and 2004, with relatively prolonged dry seasons and low total burned area values, and the inverse in 2003, suggest that the influences of the rainfall regimes dynamics are relative, whether or not linked to regional climatic anomalies. Although systematic data are not available to compute and analyze the fire causes, it is possible to infer that these variations are probably associated to different rates of influence of human ignitions. In the annual distribution of the burned areas in other tropical savanna areas, linked more strongly to core areas of the Cerrado biome, the year 2010 was also among the most affected in studies on the Serra do Tombador Natural Reserve (Daldegan et al., 2014) and in the Serra da Canastra National Park (Lemes et al., 2014). Nevertheless, the studies return a lack of convergence in other years more seriously affected by fire, showing that climatic anomalies can have an influence in this type of landscape, but they do not meet the conditions required for the fire to reach large peaks of total burned areas.

4.2. Fire over different tree cover domains and recurrence distribution analysis

A hierarchical pattern characteristic of the incidence of fire in the enclave was verified, where the subtotals of burned areas covered a larger annual percentage of surfaces with low tree cover, followed by those with medium and high tree cover, which related to the landscape configuration and the usual fire propagation behavior of the CASE. These results are in agreement with those obtained in modeling fire frequency

on different Cerrado formations in Jalapão State Park, in which the longest fire intervals were found in dense woodlands, rather than shrub and savanna areas (Pereira Júnior et al., 2014).

Higher density tree surfaces during the middle dry season fires were more significantly affected, compared to the early and out-of-dry season periods. These results further support the general hypothesis that fires in the period of greatest accumulated drought can be more aggressive against tree vegetation in savanna environments (Laris, 2002; Smit et al., 2010). The results of the regression analysis allow to infer that an increase in fire size strongly determine the increase of total woody areas affected by fire.

The analysis of tree cover domains in 2000 and 2015 by different areas of recurrence suggests that the fire affected areas may also lead to losses of medium-high and high tree cover areas in the CASE. There were no significant differences between the losses of vegetation cover in affected areas at higher or lower frequencies, but these results need to be weighted by the time scale analyzed (17 years) and by the lack of fire recurrence information from the period prior to the study. Higher fire frequencies are usually related to reduced woody vegetation cover in savanna vegetation (Smit et al., 2010) and rainforest in the south-east of Amazonia (Balch et al., 2015). On the other hand, resilient behavior in the trees of savanna-forest boundaries of the Brazilian Cerrado is reported, where tree topkill, not mortality, governs the dynamics of frequent fires (Hoffmann et al., 2009). Future studies in the CASE, in a high detailed scale, are needed to describe the relation between tree mortality rates, recurrence and severity of fire affected areas in different burning periods.

Four of the five zones of high fire recurrence identified are located near the axis of the Estanho Road, which implies a strong anthropic influence on the time series records for these areas. Information in the studies on implementing the CANP (ICMBio, 2016) specifies the anthropic pressures acting on certain areas of the CASE, leading to speculation on the causes of the registered fires. In areas of high recurrence C and D, it can be inferred that the sources of ignition are mainly linked to fire use for land preparation for agro-pastoral activities at the beginning of the series, or even criminal and/or accidental burns initiated from the road axis. In zone E, in the Igarapé Preto IL, garimpo (informal mining) activities are identified, and the fires identified are probably connected with these activities, in addition to the frequent use of fire for 'clearing areas' by the indigenous population. Both zones A and B are located within the Marmelos IL. Zone B is located near the Estanho Road, while access to zone A is more closely linked to water courses, about 35 km away from the nearest indigenous human settlement. It is speculated that at least part of the ignitions of these areas are caused by hunters, not exclusively indigenous, to attract animals. On the other hand, natural fires (from lightning) are also considered a cause of fires in these areas. Studies of other natural parks, located in the core area of the Cerrado, reveal that natural burning should be considered as an important causal factor. At Emas National Park, 41 of the 44 records identified between 1995 and 1999 were from natural ignitions, mainly small burns during the rainy season (Ramos-Neto and Pivello, 2000). As for the Chapada dos Veadeiros National Park, 12% of the fires occurring between 1992 and 2003 were caused by lightning (Fiedler et al., 2006). Increased monitoring capacity in cooperative processes with local indigenous communities will be required to obtain more accurate information on the causes of the CASE fires. Although intentional fires without the authorization of environmental agencies are a crime under national law, no results of any CASE investigation that recognizes the cause of fires are known.

4.3. Methodological progresses, limitations and perspectives

This article explored the combination of information derived from optical sensors (Landsat and MODIS surface reflectance data and VCF tree cover data) and radar (TRMM precipitation data) to analyze the spatial and temporal patterns of fire incidence in one of the biggest

savanna enclaves in the southern Brazilian Amazon. This methodology is an original approach compared to previous studies of fire incidence available in the literature, which enabled to: i) monitor the annual/seasonal fire extent and frequency on fine spatial resolution for the last 17 years by mining all available Landsat (TM, ETM+ and OLI) and complementing temporal gaps with information derived from daily MODIS surface reflectance series; ii) identify four burning periods per year in the time series based on the daily TRMM rainfall dataset; and iii) test hypotheses related to fire seasonality/recurrence and amount of burned woody vegetation using VCF tree cover layers. All remote sensing data sources used in this study are available for free and can be employed for seasonal studies of the incidence of fire in the most distinct global landscapes.

The analysis of an extensive time series of Landsat images enabled 1432 fire scars to be extracted from the CASE over the last 17 years, of which 32% were reviewed in a daily MODIS time series for correct seasonal assignment. The results obtained corroborate with other studies that have already demonstrated the potential of the MODIS series for accurate time information on burned areas (Boschetti et al., 2015; Panisset et al., 2014; Veraverbeke et al., 2014). Probable omissions of very small burned areas should also be taken into consideration, especially those <0.09 ha (one Landsat pixel), or those linked to wider gaps in the availability of images free from atmospheric disturbances during the rainy season, which are difficult to identify in the existing pre-post images comparison. Nevertheless, it is believed that the database presents a reliable picture of fire incidence in the enclave.

The seasonal subdivision, contextualized from the daily TRMM data, allowed a dynamic framing of annual burning seasons, avoiding the double incidence of error based on a static definition of these periods. With the subdivision of the four annual burning periods (out-of-dry season, early dry season, middle dry season, late dry season), it was sought to overcome the early-late dichotomy existing in many fire incidence studies in savannas (Laris et al., 2016). It is believed that the adopted subdivision feasibly captures the main generic stages of the condition of fuel loads from the predominant vegetation formations in the CASE, and is compatible with the interpretation of burning patterns. Nevertheless, future research may help to further refine these periods, based on a more exhaustive study of regional climatic characteristics that includes temperature data, evapotranspiration, wind direction patterns and even more consistent pluviometry data based on meteorological station data. With the recent inauguration of a fixed CANP base in the CASE, a local meteorological station may be available in the near future to replace the current frame in which the nearest station is about 150 km northwest (Humaitá Meteorological Station). For future CASE experimentation involving the monitoring of prescribed burns in different periods, the use of dates closer to the intersections (of the 17 years analyzed) of each period will be characterized as a good alternative for correct framing.

The use of VCF products was successful in comparing the incidence of fire on different tree cover domains, enabling the annual/seasonal quantity of areas of high predominance of tree cover affected by fire to be categorized and estimated. Using updated information every five years, it was possible to capture the dynamics of tree cover percentages in four moments of the time series. This provided an advantage over the use of a static vegetation map in the interpretation of the annual results, which is the approach used to study the annual burned areas of the Serra do Tombador Natural Reserve (Daldegan et al., 2014) and fire frequency modeling in Jalapão State Park (Pereira Júnior et al., 2014), although it is inferior in terms of detail of the existing vegetation formations.

From this study, current research lines are focused on understanding the responses of vegetation to fire in the CASE, seeking to recognize how the process of post-fire regeneration occurs in its different vegetation formations. Progress is also being made on the fusion of fine and low/moderate spatial resolution surface reflectance products in the estimation of fire severity data. These lines aim to advance methodologically

with the analysis and monitoring of the fire impacts on the Cerrado-Amazon transition areas, at the same time as adding new information to the database presented here, which will help in drafting the fire management plan and consequently with land management of the CASE.

5. Conclusion

This study explored the combination of information derived from remote sensing data sources in the generation and analysis of a fire incidence database in one of the biggest savanna enclaves in the southern Brazilian Amazon, the CASE. The applied methodology allowed the quantification and spatial categorization of the fire occurrences over the last 17 years (the entire Landsat-MODIS coincident series available), generating information on annual/seasonal variation. The discussion of the results, based on a fine spatial resolution, provides new insights into the analysis of burned areas of the neotropical savannas, and especially over the Cerrado-Amazon enclaves, spatially and statistically reinforcing important aspects linked to the seasonality patterns of fire incidence in this landscape.

In the CASE, very large fires, found mainly in the middle dry period, result in large peaks of total burned areas within the time series, especially for the years 2005, 2010 and 2014. A higher number of annual fire occurrences were not directly related to the total areas recorded, which are mostly caused by small and very small burned areas within the time series. The seasonal comparison shows that during the dry period 97.64% of the total burned areas were recorded throughout the time series. It also revealed the high magnitude of fires during the middle period, responsible for 86.21% of the total burned in 32.05% of fire occurrences. Significant differences were identified between the proportion of higher density tree cover surfaces affected by fire during the middle dry season, and contrasted with the early and out-of-dry season fires.

Conflict of interest

The authors declare that there are no conflicts of interest regarding this manuscript.

Acknowledgment

We thank the CAPES Foundation (Brazil) for the grant (process number 9540-13-0) given to the first author. We are also grateful to Bruno Contursi Cambraia and all the team of the Campos Amazônicos National Park, who provided data and encouraged the research development.

Appendix A. Supplementary data

Supplementary data to this article can be found online at <http://dx.doi.org/10.1016/j.scitotenv.2017.05.194>.

References

- ADCIF, Spanish Department of Defense Against Forest Fires, 2017. General forest fire statistics. http://www.mapama.gob.es/es/desarrollo-rural/estadisticas/Incendios_default.aspx (accessed 13.01.17).
- Alencar, A., Asner, G.P., Knapp, D., Zarin, D., 2011. Temporal variability of forest fires in eastern Amazonia. *Ecol. Appl.* 21:2397–2412. <http://dx.doi.org/10.1890/10-1168.1>.
- Alencar, A.A., Brando, P.M., Asner, G.P., Putz, F.E., 2015. Landscape fragmentation, severe drought and the new Amazon forest fire regime. *Ecol. Appl.* 25:1493–1505. <http://dx.doi.org/10.1017/CBO9781107415324.004>.
- Andersen, A.N., Cook, G.D., Corbett, L.K., Douglas, M.M., Eager, R.W., Russell-Smith, J., Setterfield, S.A., Williams, R.J., Woinarski, J.C.Z., 2005. Fire frequency and biodiversity conservation in Australian tropical savannas: implications from the Kapalga fire experiment. *Austral. Ecol.* 30:155–167. <http://dx.doi.org/10.1111/j.1442-9993.2005.01441.x>.
- Aragão, L.E.O.C., Malhi, Y., Barbier, N., Lima, A., Shimabukuro, Y.E., Anderson, L., Saatchi, S., 2008. Interactions between rainfall, deforestation and fires during recent years in the Brazilian Amazonia. *Philos. Trans. R. Soc. Lond. Ser. B Biol. Sci.* 363:1779–1785. <http://dx.doi.org/10.1098/rstb.2007.0026>.
- Asner, G.P., 2001. Cloud cover in Landsat observations of the Brazilian Amazon. *Int. J. Remote Sens.* 22:3855–3862. <http://dx.doi.org/10.1080/01431160010006926>.

- Balch, J.K., Brando, P.M., Nepstad, D.C., Coe, M.T., Silvério, D., Massad, T.J., Davidson, E.A., Lefebvre, P., Oliveira-Santos, C., Rocha, W., Cury, R.T.S., Parsons, A., Carvalho, K.S., 2015. The susceptibility of southeastern Amazon forests to fire: insights from a large-scale burn experiment. *Bioscience* 65:893–905. <http://dx.doi.org/10.1093/biosci/biv106>.
- Bastarrika, A., Chuvieco, E., Martín, M.P., 2011. Mapping burned areas from Landsat TM/ETM+ data with a two-phase algorithm: balancing omission and commission errors. *Remote Sens. Environ.* 115:1003–1012. <http://dx.doi.org/10.1016/j.rse.2010.12.005>.
- Bastarrika, A., Alvarado, M., Artano, K., Martínez, M.P., Mesanza, A., Torre, L., Ramo, R., Chuvieco, E., 2014. BAMS: a tool for supervised burned area mapping using Landsat data. *Remote Sens.* 6:12360–12380. <http://dx.doi.org/10.3390/rs61212360>.
- Bond, W.J., Woodward, F.I., Midgley, G.F., 2005. The global distribution of ecosystems in a world without fire. *New Phytol.* 165:525–538. <http://dx.doi.org/10.1111/j.1469-8137.2004.01252.x>.
- Boschetti, L., Roy, D.P., Justice, C.O., Humber, M.L., 2015. MODIS–Landsat fusion for large area 30 m burned area mapping. *Remote Sens. Environ.* 161:27–42. <http://dx.doi.org/10.1016/j.rse.2015.01.022>.
- Bowman, D.M.J.S., Zhang, Y., Walsh, A., Williams, R.J., 2003. Experimental comparison of four remote sensing techniques to map tropical savanna fire-scars using Landsat-TM imagery. *Int. J. Wildland Fire* 12:341. <http://dx.doi.org/10.1071/WF03030>.
- Bowman, D.M.J.S., Balch, J.K., Artaxo, P., Bond, W.J., Carlson, J.M., Cochrane, M.A., Antonio, C.M.D., Defries, R.S., Doyle, J.C., Harrison, S.P., Johnston, F.H., Keeley, J.E., Krawchuk, M.A., Kull, C.A., Marston, J.B., Moritz, M.A., Prentice, I.C., Roos, C.I., Scott, A.C., Swetnam, T.W., van der Werf, G.R., Pyne, S.J., 2010. Fire in the Earth System. *Science* (80-) 481. <http://dx.doi.org/10.1126/science.1163886>.
- Carneiro Filho, A., 1993. Cerrados amazônicos: fósseis vivos? Algumas reflexões. *Rev. do Inst. Geológico* 14:63–68. <http://dx.doi.org/10.5935/0100-929X.19930010>.
- Cavalcanti, R.B., Joly, C.A., 2002. Biodiversity and conservation priorities in the Cerrado region. In: Oliveira, P.S., Marquis, R.J. (Eds.), *The Cerrados of Brazil: Ecology and Natural History of a Neotropical Savanna*. Columbia University Press, New York, EUA, pp. 351–367.
- Certini, G., 2005. Effects of fire on properties of forest soils: a review. *Oecologia* 143:1–10. <http://dx.doi.org/10.1007/s00442-004-1788-8>.
- CFS, Canadian Forest Service, 2017. Canadian Wildland Fire Information System. <http://cwifis.cfs.nrcan.gc.ca/home> (accessed 13.01.17).
- Chen, Y., Randerson, J.T., Morton, D.C., Defries, R.S., Collatz, G.J., Kasibhatla, P.S., Giglio, L., Jin, Y., Marlier, M.E., 2011. Forecasting fire season severity in South America using sea surface temperature anomalies. *Science* (80) 334:787–792. <http://dx.doi.org/10.1126/science.1208898>.
- Chen, Y., Morton, D.C., Jin, Y., Collatz, G.J., Kasibhatla, P.S., van der Werf, G.R., Defries, R.S., Randerson, J.T., 2013. Long-term trends and interannual variability of forest, savanna and agricultural fires in South America. *Carbon Manage.* 4:617–638. <http://dx.doi.org/10.4155/cmt.13.61>.
- Chuvieco, E., Aguado, I., Yebra, M., Nieto, H., Salas, J., Martín, M.P., Vilar, L., Martínez, J., Martín, S., Ibarra, P., de la Riva, J., Baeza, J., Rodríguez, F., Molina, J.R., Herrera, M.A., Zamora, R., 2010. Development of a framework for fire risk assessment using remote sensing and geographic information system technologies. *Ecol. Model.* 221:46–58. <http://dx.doi.org/10.1016/j.ecolmodel.2008.11.017>.
- Daldegan, G.A., de Carvalho Júnior, O.A., Guimarães, R.F., Gomes, R.A.T., de Ribeiro, F., McManus, C., 2014. Spatial patterns of fire recurrence using remote sensing and GIS in the Brazilian savanna: Serra do Tombador Nature Reserve, Brazil. *Remote Sens.* 6:9873–9894. <http://dx.doi.org/10.3390/rs6109873>.
- D'Amico, A.R., 2014. Avaliação da interferência do fogo na ocorrência de mamíferos de médio e grande porte no enclave de cerrado do Parque Nacional dos Campos Amazônicos. ICMBio; Porto Velho, Rondônia, Brazil.
- Dantas, V. de L., Batalha, M.A., Pausas, J.G., 2013. Fire drives functional thresholds on the savanna–forest transition. *Ecology* 94:2454–2463. <http://dx.doi.org/10.1890/12-1629.1>.
- Durigan, G., Ratter, J.A., 2016. The need for a consistent fire policy for Cerrado conservation. *J. Appl. Ecol.* 53:11–15. <http://dx.doi.org/10.1111/1365-2664.12559>.
- Eidenshink, J., Schwind, B., Brewer, K., Zhu, Z., Quayle, B., Howard, S., 2007. A project for monitoring trends in burn severity. *Fire Ecol.* 3:3–21. <http://dx.doi.org/10.4996/fireecology.0301003>.
- Eva, H., Lambin, E.F., 2000. Fires and land-cover change in the tropics: a remote sensing analysis at the landscape scale. *J. Biogeogr.* 27:765–776. <http://dx.doi.org/10.1046/j.1365-2699.2000.00441.x>.
- Fiedler, N.C., Merlo, D.A., Medeiros, M.B., 2006. Ocorrência de incêndios florestais no Parque Nacional da Chapada dos Veadeiros, Goiás. *Ciência Florestal* 16, 153–161.
- Fraser, R.H., Li, Z., Landry, R., 2000. SPOT-VEGETATION for characterizing boreal forest fires. *Int. J. Remote Sens.* 21, 3525–3532.
- Fu, R., Yin, L., Li, W., Arias, P.A., Dickinson, R.E., Huang, L., Chakraborty, S., Fernandes, K., Liebmann, B., Fisher, R., Myneni, R.B., 2013. Increased dry-season length over southern Amazonia in recent decades and its implication for future climate projection. *Proc. Natl. Acad. Sci.* 110:18110–18115. <http://dx.doi.org/10.1073/pnas.1302584110>.
- Giglio, L., Randerson, J.T., Van Der Werf, G.R., Kasibhatla, P.S., Collatz, G.J., Morton, D.C., Defries, R.S., 2010. Assessing variability and long-term trends in burned area by merging multiple satellite fire products. *Biogeosciences* 7:1171–1186. <http://dx.doi.org/10.5194/bg-7-1171-2010>.
- Giglio, L., Randerson, J.T., Van Der Werf, G.R., 2013. Analysis of daily, monthly, and annual burned area using the fourth-generation global fire emissions database (GFED4). *J. Geophys. Res. Biogeosci.* 118:317–328. <http://dx.doi.org/10.1002/jgrg.20042>.
- Goldammer, J.G., 1993. Historical biogeography of fire: tropical and subtropical. *The Ecological, Atmospheric and Climatic Importance of Vegetation Fires*. John Wiley & Sons, Ltd, New York, pp. 297–314.
- Greenville, A.C., Dickman, C.R., Wardle, G.M., Letnic, M., 2009. The fire history of an arid grassland: the influence of antecedent rainfall and ENSO. *Int. J. Wildland Fire* 18: 631–639. <http://dx.doi.org/10.1071/WF08093>.
- Hardesty, J., Myers, R., Fulks, W., 2005. Fire, ecosystems and people: a preliminary assessment of fire as a global conservation issue. *Fire Manage.* 22, 78–87.
- Hayes, D.J., Cohen, W.B., 2007. Spatial, spectral and temporal patterns of tropical forest cover change as observed with multiple scales of optical satellite data. *Remote Sens. Environ.* 106:1–16. <http://dx.doi.org/10.1016/j.rse.2006.07.002>.
- Hoffmann, W.A., Moreira, A.G., 2002. The role of fire in population dynamics of woody plants. In: Oliveira, P.S., Marquis, R.J. (Eds.), *The Cerrados of Brazil: Ecology and Natural History of a Neotropical Savanna*. Columbia University Press, New York, EUA, pp. 139–177.
- Hoffmann, W.A., Adasme, R., Haridasan, M., De Carvalho, M.T., Geiger, E.L., Pereira, M.A.B., Gotsch, S.G., Franco, A.C., 2009. Tree topkill, not mortality, governs the dynamics of savanna-forest boundaries under frequent fire in central Brazil. *Ecology* 90: 1326–1337. <http://dx.doi.org/10.1890/08-0741.1>.
- Hudak, A.T., Brockett, B.H., 2004. Mapping fire scars in a southern African savannah using Landsat imagery. *Int. J. Remote Sens.* 25:3231–3243. <http://dx.doi.org/10.1080/01431160310001632666>.
- Huffman, G.J., Bolvin, D.T., Nelkin, E.J., Wolff, D.B., Adler, R.F., Gu, G., Hong, Y., Bowman, K.P., Stocker, E.F., 2007. The TRMM Multisatellite Precipitation Analysis (TMPA): quasi-global, multiyear, combined-sensor precipitation estimates at fine scales. *J. Hydrometeorol.* 8:38–55. <http://dx.doi.org/10.1175/JHM560.1>.
- ICMBio, Chico Mendes Institute for Biodiversity Conservation, 2016. Plano de Manejo - Parque Nacional dos Campos Amazônicos (Brasília, Brasil).
- ICNF, Institute for Nature Conservation and Forests of Portugal, 2017. Cartografia nacional de áreas ardidas. <http://www.icnf.pt/portal/florestas/dfici/inc/info-geo> (accessed 13.01.17).
- INPE, National Institute For Space Research, 2017. Portal for the monitoring of vegetation fires (Queimadas Project). <http://www.inpe.br/queimadas/> (accessed 01.20.17).
- Jacquín, A., Goulard, M., 2013. Using spatial statistics tools on remote-sensing data to identify fire regime linked with savanna vegetation degradation. *Int. J. Agric. Environ. Inf. Syst.* 4:68–82. <http://dx.doi.org/10.4018/jaeis.2013010105>.
- Kampstra, P., 2008. Beanplot: a boxplot alternative for visual comparison of distributions. *J. Stat. Softw.* 28:1–9. <http://dx.doi.org/10.18637/jss.v028.c01>.
- Kaufman, Y.J., Wald, A.E., Remer, L.A., Gao, B.-C., Li, R.-R., Flynn, L., 1997. The MODIS 2.1 channel-correlation with visible reflectance for use in remote sensing of aerosol. *IEEE Trans. Geosci. Remote Sens.* 35:1286–1298. <http://dx.doi.org/10.1109/36.628795>.
- Key, C.H., Benson, N.C., 2006. Landscape assessment (LA): sampling and analysis methods. In: Lutes, D.C., Keane, R.E., Caratti, J.F., Key, C.H., Benson, N.C., Sutherland, S., Gangi, L.J. (Eds.), *FIREMON: Fire Effects Monitoring and Inventory System*. U.S. Department of Agriculture, Forest Service, Rocky Mountain Research Station, Fort Collins, CO, USA, pp. 1–55.
- Killick, R., Eckley, I., 2013. changepoint: an R package for changepoint analysis. *J. Stat. Softw.* 58, 1–15.
- Kruschke, J.K., 2012. Bayesian estimation supersedes the t test. *J. Exp. Psychol. Gen.* 142: 573–603. <http://dx.doi.org/10.1037/a0029146>.
- Laris, P., 2002. Burning the seasonal mosaic: preventative burning strategies in the wooded savanna of southern Mali. *Hum. Ecol.* 30:155–186. <http://dx.doi.org/10.1023/A:1015685529180>.
- Laris, P., 2005. Spatiotemporal problems with detecting and mapping mosaic fire regimes with coarse-resolution satellite data in savanna environments. *Remote Sens. Environ.* 99:412–424. <http://dx.doi.org/10.1016/j.rse.2005.09.012>.
- Laris, P., Koné, M., Dadashi, S., Dembele, F., 2016. The early/late fire dichotomy: time for a reassessment of Aubréville's savanna fire experiments. *Prog. Phys. Geogr.* 41:68–94. <http://dx.doi.org/10.1177/0309133316665570>.
- Ledru, M.P., 2002. Late Quaternary history and evolution of the Cerrados as revealed by palynological records. In: Oliveira, P.S., Marquis, R.J. (Eds.), *The Cerrados of Brazil: Ecology and Natural History of a Neotropical Savanna*. Columbia University Press, New York, EUA, pp. 33–50.
- Lemes, G.P., Maticardi, E.A.T., Costa, O.B., Leal, F.A., 2014. Spatiotemporal assessment of forest fires occurred in the Serra da Canastra National Park between 1991 and 2011. *Ambiência* 10:247–266. <http://dx.doi.org/10.5935/ambiencia.2014supl03>.
- Lentile, L.B., Holden, Z.A., Smith, A.M.S., Falkowski, M.J., Hudak, A.T., Morgan, P., Lewis, S.A., Gessler, P.E., Benson, N.C., 2006. Remote sensing techniques to assess active fire characteristics and post-fire effects. *Int. J. Wildland Fire* 15:319–345. <http://dx.doi.org/10.1071/WF05097>.
- Levin, N., Heimowitz, A., 2012. Mapping spatial and temporal patterns of Mediterranean wildfires from MODIS. *Remote Sens. Environ.* 126:12–26. <http://dx.doi.org/10.1016/j.rse.2012.08.003>.
- Levine, J.S., Cofer, W.R., Cahoon, D.J., Winstead, E.L., 1995. Biomass burning – a driver for global change. *Environ. Sci. Technol.* 29, 120–125.
- Lewis, S.L., Brando, P.M., Phillips, O.L., van der Heijden, G.M.F., Nepstad, D., 2011. The 2010 Amazon drought. *Science* 331:554. <http://dx.doi.org/10.1126/science.1200807>.
- Libonati, R., DaCamara, C.C., Setzer, A.W., Morelli, F., de Jesus, S.C., Candido, P.A., Melchiori, A.E., 2014. Validation of the burned area '(VW)' Modis algorithm in Brazil. In: Viegas, D.X. (Ed.), *Advances in Forest Fire Research*. Universidade de Coimbra, Coimbra, Portugal, pp. 1774–1789.
- Libonati, R., DaCamara, C., Setzer, A., Morelli, F., Melchiori, A., 2015. An algorithm for burned area detection in the Brazilian Cerrado using 4 µm MODIS imagery. *Remote Sens.* 7:15782–15803. <http://dx.doi.org/10.3390/rs71115782>.
- Maeda, E.E., Formaggio, A.R., Shimabukuro, Y.E., Arcoverde, G.F.B., Hansen, M.C., 2009. Predicting forest fire in the Brazilian Amazon using MODIS imagery and artificial neural networks. *Int. J. Appl. Earth Obs. Geoinf.* 11:265–272. <http://dx.doi.org/10.1016/j.jag.2009.03.003>.
- Marengo, J.A., Liebmann, B., Kousky, V.E., Filizola, N.P., Wainer, I.C., 2001. Onset and end of the rainy season in the Brazilian Amazon Basin. *J. Clim.* 14:833–852. [http://dx.doi.org/10.1175/1520-0442\(2001\)014<0833:OAEOTR>2.0.CO;2](http://dx.doi.org/10.1175/1520-0442(2001)014<0833:OAEOTR>2.0.CO;2).
- Marengo, J.A., Nobre, C.A., Tomasella, J., Oyama, M.D., de Oliveira, G.S., de Oliveira, R., Camargo, H., Alves, L.M., Brown, I.F., 2008. The drought of Amazonia in 2005. *J. Clim.* 21:495–516. <http://dx.doi.org/10.1175/2007JCLI1600.1>.

- Marengo, J.A., Tomasella, J., Alves, L.M., Soares, W.R., Rodriguez, D.A., 2011. The drought of 2010 in the context of historical droughts in the Amazon region. *Geophys. Res. Lett.* 38:1–5. <http://dx.doi.org/10.1029/2011GL047436>.
- Masek, J.G., Vermote, E.F., Saleous, N.E., Wolfe, R., Hall, F.G., Huemmrich, K.F., Gao, F., Kutler, J., Lim, T., 2006. A Landsat surface reflectance dataset for North America, 1990–2000. *IEEE Geosci. Remote Sens. Lett.* 3:68–72. <http://dx.doi.org/10.1109/LGRS.2005.857030>.
- Melchiori, A.E., Setzer, A.W., Morelli, F., Libonati, R., Cândido, P. de A., de Jesus, S.C., 2014. A Landsat-TM/OLI algorithm for burned areas in the Brazilian Cerrado: preliminary results. In: Viegas, D.X. (Ed.), *Advances in Forest Fire Research*. Coimbra University Press, Coimbra, Portugal, pp. 23–30.
- Miranda, H.S., Sato, M.N., Nascimento Neto, W., Aires, F.S., 2009. Fires in the Cerrado, the Brazilian savanna. In: Cochran, M.A. (Ed.), *Tropical Fire Ecology: Climate Change, Land Use, and Ecosystem Dynamics*. Springer, Berlin Heidelberg, Chichester, UK, pp. 427–450.
- Moreira, A.G., 2000. Effects of fire protection on savanna structure in central Brazil. *J. Biogeogr.* 27:1021–1029. <http://dx.doi.org/10.1046/j.1365-2699.2000.00422.x>.
- Moreno, M.V., Conedera, M., Chuvieco, E., Pezzatti, G.B., 2014. Fire regime changes and major driving forces in Spain from 1968 to 2010. *Environ. Sci. Pol.* 37:11–22. <http://dx.doi.org/10.1016/j.envsci.2013.08.005>.
- Morton, D.C., DeFries, R.S., Nagol, J., Souza Jr., C.M., Kasischke, E.S., Hurr, G.C., Dubayah, R., 2011. Mapping canopy damage from understory fires in Amazon forests using annual time series of Landsat and MODIS data. *Remote Sens. Environ.* 115:1706–1720. <http://dx.doi.org/10.1016/j.rse.2011.03.002>.
- Motta, P.E.F., Curi, N., Franzmeier, D.F., 2002. Relation of soils and geomorphic surfaces in the Brazilian Cerrado. In: Oliveira, P.S., Marquis, R.J. (Eds.), *The Cerrados of Brazil: Ecology and Natural History of a Neotropical Savanna*. Columbia University Press, New York, USA, pp. 13–32.
- Nepstad, D., Lefebvre, P., Lopes da Silva, U., Tomasella, J., Schlesinger, P., Solorzano, L., Moutinho, P., Ray, D., Guerreira Benito, J., 2004. Amazon drought and its implications for forest flammability and tree growth: a basin-wide analysis. *Glob. Chang. Biol.* 10:704–717. <http://dx.doi.org/10.1111/j.1529-8817.2003.00772.x>.
- Oliveira-Filho, A.T., Ratter, J.A., 2002. Vegetation physiognomies and woody flora of the Cerrado biome. In: Oliveira, P.S., Marquis, R.J. (Eds.), *The Cerrados of Brazil: Ecology and Natural History of a Neotropical Savanna*. Columbia University Press, New York, USA, pp. 91–120.
- Ometto, J.P., Souza-Neto, E.R., Tejada, G., 2016. Land use, land cover and land use change in Brazilian Amazon (1960–2013). In: Nagy, L., Forsberg, B.R., Artaxo, P. (Eds.), *Interactions Between Biosphere, Atmosphere and Human Land Use Amazon Basin, Ecological Studies*. Springer, Berlin Heidelberg, Berlin, Heidelberg. <http://dx.doi.org/10.1007/978-3-662-49902-3>.
- Padilla, M., Stehman, S.V., Ramo, R., Corti, D., Hantson, S., Oliva, P., Alonso-Canas, I., Bradley, A.V., Tansey, K., Mota, B., Pereira, J.M., Chuvieco, E., 2015. Comparing the accuracies of remote sensing global burned area products using stratified random sampling and estimation. *Remote Sens. Environ.* 160:114–121. <http://dx.doi.org/10.1016/j.rse.2015.01.005>.
- Panisset, J., Libonati, R., DaCamara, C.C., Barros, A., 2014. Assigning dates to burned areas in Portugal based on NIR and the reflected component of MIR as derived from MODIS. In: Viegas, D.X. (Ed.), *Advances in Forest Fire Research*. Coimbra University Press, Coimbra, Portugal, pp. 23–30.
- Pausas, J.G., Keeley, J.E., 2009. A burning story: the role of fire in the history of life. *Bioscience* 59:593–601. <http://dx.doi.org/10.1525/bio.2009.59.7.10>.
- Pereira, J.M.C., 2003. Remote sensing of burned areas in tropical savannas. *Int. J. Wildland Fire* 12:259. <http://dx.doi.org/10.1071/WF03028>.
- Pereira Júnior, A.C., Oliveira, S.L.J., Pereira, J.M.C., Turkman, M.A.A., 2014. Modelling fire frequency in a Cerrado savanna protected area. *PLoS One*:9. <http://dx.doi.org/10.1371/journal.pone.0102380>.
- Phillips, N., 2017. 'yarr' R package. <https://cran.r-project.org/web/packages/yarr/index.html> (accessed 02.17.17).
- Pivello, V.R., 2011. The use of fire in the Cerrado and Amazonian rainforests of Brazil: past and present. *Fire Ecol.* 7:24–39. <http://dx.doi.org/10.4996/fireecology.0701024>.
- Ramos-Neto, M.B., Pivello, V.R., 2000. Lightning fires in a Brazilian Savanna National Park: rethinking management strategies. *Environ. Manag.* 26:675–684. <http://dx.doi.org/10.1007/s002670010124>.
- Ratter, J.A., Bridgewater, S., Ribeiro, J.F., 2003. Analysis of the floristic composition of the Brazilian cerrado vegetation: comparison of the woody vegetation of 376 areas. *Edinb. J. Bot.* 57–109.
- RCT, R Core Team, 2016. R: a language and environment for statistical computing. <https://www.r-project.org/> (accessed 09.01.16).
- Röder, A., Hill, J., Duguay, B., Alloza, J.A., Vallejo, R., 2008. Using long time series of Landsat data to monitor fire events and post-fire dynamics and identify driving factors - a case study in the Ayora region (eastern Spain). *Remote Sens. Environ.* 112:259–273. <http://dx.doi.org/10.1016/j.rse.2007.05.001>.
- Russel-Smith, J., Ryan, P.G., Durieu, R., 1997. A Landsat MSS-derived fire history of Kakadu National Park, monsoonal northern Australia, 1980–94: seasonal extent, frequency and patchiness. *J. Appl. Ecol.* 34, 748–766.
- Salgado-Labouriau, M.L., Ferraz-Vicentini, K.R., 1994. Fire in the Cerrado 32,000 years ago. *Curr. Res. Pleistocene* 11, 85–87.
- Sano, E.E., Ferreira, L.G., Asner, G.P., Steinke, E.T., 2007. Spatial and temporal probabilities of obtaining cloud-free Landsat images over the Brazilian tropical savanna. *Int. J. Remote Sens.* 28:2739–2752. <http://dx.doi.org/10.1080/01431160600981517>.
- Schroeder, W., Prins, E., Giglio, L., Csiszar, I., Schmidt, C., Morissette, J., Morton, D., 2008. Validation of GOES and MODIS active fire detection products using ASTER and ETM+ data. *Remote Sens. Environ.* 112:2711–2726. <http://dx.doi.org/10.1016/j.rse.2008.01.005>.
- Schroeder, W., Alencar, A., Arima, E.Y., Setzer, A., 2009. The spatial distribution and inter-annual variability of fire in Amazonia. *Amaz. Glob. Chang.* 43–60. <http://dx.doi.org/10.1029/2008GM000723>.
- Schroeder, W., Csiszar, I., Giglio, L., Schmidt, C.C., 2010. On the use of fire radiative power, area, and temperature estimates to characterize biomass burning via moderate to coarse spatial resolution remote sensing data in the Brazilian Amazon. *J. Geophys. Res.* 115:1–10. <http://dx.doi.org/10.1029/2009JDO13769>.
- Senf, C., Leitão, P.J., Dirk, P., Van Der Linden, S., Hostert, P., 2015. Mapping land cover in complex Mediterranean landscapes using Landsat: improved classification accuracies from integrating multi-seasonal and synthetic imagery. *Remote Sens. Environ.* 156, 527–536.
- Sexton, J.O., Song, X.-P., Feng, M., Noojipady, P., Anand, A., Huang, C., Kim, D.-H., Collins, K.M., Channan, S., Dimiceli, C., Townshend, J.R., 2013. Global, 30-m resolution continuous fields of tree cover: Landsat-based rescaling of MODIS Vegetation Continuous Fields with Lidar-based estimates of error. *Int. J. Digit. Earth* 8947. <http://dx.doi.org/10.1080/17538947.2013.786146> (130321031236007).
- Shimabukuro, Y.E., Miettinen, J., Beuchle, R., Grecchi, R.C., Simonetti, D., Achard, F., 2015. Estimating burned area in Mato Grosso, Brazil, using an object-based classification method on a systematic sample of medium resolution satellite images. *IEEE J. Sel. Top. Appl. Earth Obs. Remote Sens.* 8, 4502–4508.
- Silva Cardozo, F. da, Shimabukuro, Y.E., Pereira, G., Silva, F.B., 2011. Using remote sensing products for environmental analysis in South America. *Remote Sens.* 3:2110–2127. <http://dx.doi.org/10.3390/rs3102110>.
- Silveira, L., de Almeida Jacomo, A.T., Diniz Filho, J.A.F., Rodrigues, F.H.G., 1999. Impact of wildfires on the megafauna of Emas National Park, central Brazil. *Oryx* 33:108–114. <http://dx.doi.org/10.1046/j.1365-3008.1999.00039.x>.
- Smit, I.P.J., Asner, G.P., Govender, N., Kennedy-Bowdoin, T., Knapp, D.E., Jacobson, J., 2010. Effects of fire on woody vegetation structure in African savanna. *Ecol. Appl.* 20:1865–1875. <http://dx.doi.org/10.1890/09-0929.1>.
- Trigg, S., Flasse, S., 2000. Characterizing the spectral-temporal response of burned savannah using in situ spectroradiometry and infrared thermometry. *Int. J. Remote Sens.* 21:3161–3168. <http://dx.doi.org/10.1080/01431160050145045>.
- USGS, United States Geological Survey, 2016a. Provisional Landsat 4–7 Surface Reflectance Product Guide - v. 6.9. <http://dx.doi.org/10.1080/1073161X.1994.10467258>.
- USGS, United States Geological Survey, 2016b. Provisional Landsat 8 Surface Reflectance Code (LaSRC) Product Guide - v. 3.3. <http://dx.doi.org/10.1080/1073161X.1994.10467258>.
- USGS, United States Geological Survey, NASA, National Aeronautics and Space Administration, 2010. Global Land Survey (GLS) dataset. <https://landsat.usgs.gov/global-land-surveys-gls> (accessed 02.18.16).
- USGS, United States Geological Survey, USDA, United States Department of Agriculture Forest Service, 2017. Monitoring Trends in Burn Severity (MTSB). <http://www.mtbs.gov/> (accessed 13.01.17).
- Van Leeuwen, W.J.D., Casady, G.M., Neary, D.G., Bautista, S., Alloza, J.A., Carmel, Y., Wittenberg, L., Malkinson, D., Orr, B.J., 2010. Monitoring post-wildfire vegetation response with remotely sensed time-series data in Spain, USA and Israel. *Int. J. Wildland Fire* 19:75. <http://dx.doi.org/10.1071/WF08078>.
- Veraverbeke, S., Sedano, F., Hook, S.J., Randerson, J.T., Jin, Y., Rogers, B.M., 2014. Mapping the daily progression of large wildland fires using MODIS active fire data. *Int. J. Wildl. Fire* 23:655. <http://dx.doi.org/10.1071/WF13015>.
- Vermote, E., Wolfe, R., 2015a. MOD09GQ MODIS/Terra Surface Reflectance Daily L2G Global 250m SIN Grid V006. <http://dx.doi.org/10.5067/MODIS/MOD09GQ.006>.
- Vermote, E., Wolfe, R., 2015b. MYD09GQ MODIS/Aqua Surface Reflectance Daily L2G Global 250m SIN grid V006. <http://dx.doi.org/10.5067/MODIS/MYD09GQ.006>.
- Vermote, E.F., El Saleous, N., Justice, C.O., Kaufman, Y.J., Privette, J.L., Remer, L., Roger, J.C., Tanré, D., 1997. Atmospheric correction of visible to middle-infrared EOS-MODIS data over land surfaces: background, operational algorithm and validation. *J. Geophys. Res.* 102:17131. <http://dx.doi.org/10.1029/97JD00201>.
- Williams, R., Gill, A.M., Moore, P.H., 1998. Seasonal changes in fire behaviour in a tropical savanna in Northern Australia. *Int. J. Wildland Fire* 227–239.
- Yan, F., Wu, B., Wang, Y., 2015. Estimating spatiotemporal patterns of aboveground biomass using Landsat TM and MODIS images in the Mu Us Sandy Land, China. *Agric. For. Meteorol.* 200, 119–128.